UPWARD COCURRENT GAS-LIQUID

TWO-PHASE FLOW IN

VERTICAL TUBES

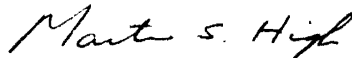By

NAMBI SHANMUGAM

Bachelor of Technology

Bharathiar University

Coimbatore, India

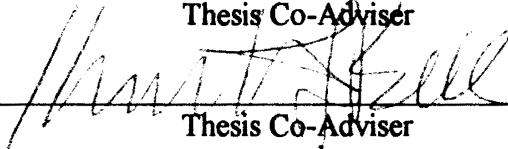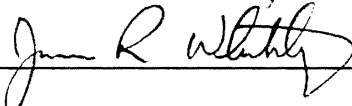1992

Submitted to the Faculty of the
Graduate College of the
Oklahoma State University
in partial fulfillment of
the requirements for
the Degree of
MASTER OF SCIENCE
May, 1994

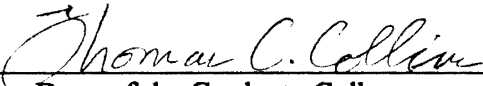UPWARD COCURRENT GAS-LIQUID

TWO-PHASE FLOW IN

VERTICAL TUBES

Thesis Approved :

Mart S. High

Thesis Co-Adviser

Thesis Co-Adviser

Dean of the Graduate College

ACKNOWLEDGMENTS

TABLE OF CONTENTS

LIST OF TABLES

vi

LIST OF FIGURES

NOMENCLATURE

D — diameter of the tube, ft.

f — friction factor, dimensionless.

g — acceleration due to gravity, ft/s^2.

g_c — gravitational constant, $= 32.2\ lb_m\text{-ft/}lb_f\text{-s}^2$.

G — mass velocity, lb/ft^2-s.

Ku — Kutateladze Number as defined by Equation (8), dimensionless.

l — length of the tube, ft.

$\dot{m}$ — mass flow rate, lb/s.

P — pressure, lb_f/ft^2.

R_v — void fraction, dimensionless.

R_l — volume fraction of the liquid in the holdup, $(1-R_v)$, dimensionless.

Re — Reynolds number, dimensionless.

s — slip, (ratio is dimensionless, velocity is in ft/s) as defined in equations (2) and (3).

S — area of cross section of the tube, ft^2.

U_m — mixture velocity, i.e. the sum of the superficial velocities of the two phases, m/s

v — velocity, ft/s.

v_g^* — modified Froude Number as presented in Equation (7), dimensionless.

$\dot{V}$ — volumetric flow rate, ft^3/s.

x — quality, dimensionless.

Subscripts

eff - effective

f - frictional

g - gas phase, gravitational

i - inner

l - liquid phase

r - ratio

t - turbulent

T - total

TPF - two-phase flow

v - velocity

Greek letters

ρ - density, lb/ft^3.

μ - viscosity, lb/ft-s.

χ, X - Martinelli parameters, dimensionless.

Φ - multiplier used in the Martinelli-Nelson correlation, dimensionless.

θ - Angle of inclination of the conduit from the vertical, degrees.

CHAPTER I

INTRODUCTION

Two-phase flow is defined as the flow of a mixture of two homogeneous phases

through a system. The general subject of two-phase flow is extremely broad and its

different facets include solid-liquid, liquid-liquid and gas-solid flows as well as gas-liquid

flow with which this work is specifically concerned. More specifically, this study has been

devoted to upward cocurrent gas-liquid two-phase flow in a vertical tube.

Two-phase gas-liquid flow occurs extensively throughout the petrochemical and

chemical process industries. To cite a few examples, it commonly occurs in boilers,

chemical reactors, condensers, distillation columns, evaporators, gas-lift pumps,

geothermal wells, oil wells, gas pipelines, refrigerators, etc. However, the nuclear power

industry is the major motivation for extensive studies on gas-liquid two-phase flow.

Significance of Phenomenological Investigations on Two-phase Flow

Gas-liquid two-phase flow differs substantially from single phase flow in that they

have different hydrodynamics as well as heat and mass transfer mechanisms. The flow

pattern of two-phase flow cannot just be described as laminar or turbulent due to the

presence of an interface between the two phases. There has been a consensus among the

researchers that the flow patterns or flow regimes of gas-liquid two-phase flow could be

classified based on the distribution of the two phases across the cross-section of the tube.

The most commonly accepted flow patterns of the vertical gas-liquid two-phase flow are

called bubbly, slug and the annular flow regimes. At a constant liquid flow rate, these flow patterns occur with increasing gas flow rate in the order mentioned above. The classification of flow patterns is essential to effectively model each of the flow regimes. These flow regimes typically have distinct flow characteristics and heat and mass transfer mechanisms. This kind of modeling, where each flow pattern is considered separately, has led to correlations that predict the associated parameters, such as the liquid to gas volume ratio and the frictional pressure drop along the tube, with greater accuracy. A detailed description of the different flow patterns and the related correlations are presented in Chapter II.

The presence of a relative motion between the two phases is another major reason for the increased number of parameters required to characterize two-phase flow. Normally, the fluid which has a lower density of the two would travel faster and would slip past the fluid with a higher density. This characteristic phenomenon led to the introduction of the term "void fraction," which is a parameter required to describe the gas-liquid two-phase flow, and can be defined as the "in situ" volume fraction of the gas phase in the two-phase system. As a result of the relative motion between the two fluids, the actual void fraction of the two-phase system and the volume fraction of the gas phase calculated from the volumetric flow rates of the two fluids are not equal. The relative motion between the two fluids also results in considerable interfacial friction which consequentially increases the total pressure drop of the fluid along the flow section. An estimate of the void fraction and the pressure drop during two-phase flow could only be obtained by a detailed study of the phenomenological behavior of two-phase fluid flow.

The above discussion makes it obvious that the relationships between pressure drop and the related variables will be much more complex for a two-phase flow than for a single phase flow. However, the perspective of two-phase flow as an intrinsically complex phenomenon would perhaps become invalid, and the importance of the two-phase flow investigations would seem boundless if one considers the eccentricity of investment the

industry has to make for constructing and maintaining equipment in which two-phase flow is expected to occur. As most of the equipment in chemical and related industries involves two-phase flow systems, the phenomenon has been given serious consideration.

Objectives of This Work

The primary goal of this project was to perform a study oriented towards solving the variety of problems faced in the prediction of two-phase flow parameters. The hydrodynamics of the two-phase flow has to be studied to better understand the heat and mass transfer mechanisms involved during two-phase flow. For performing such a study, an experimental setup had to be constructed. Design methods had to be used that would permit visual studies on the flow patterns of the two-phase flow and allow the measurement of parameters such as the void fraction of the flow and the pressure drop along the vertical test section. On completion of the construction of the apparatus, experiments had to be performed to obtain data on the flow regimes, void fractions, and the pressure drop. With the experimental results, flow pattern maps that would predict the flow regime given the superficial mass flow rates of the two fluids, figures that would be able to predict the void fraction and the total pressure drop of the two-phase flow were planned to be developed. Finally, appropriate recommendations for future work were intended to be provided.

The results of this heuristic work were planned to be used as a first step to further the investigations on the seemingly perplexing two-phase flow phenomenon.

Thesis Organization

This thesis has been organized in the order the objectives were met. A meticulous survey has been performed on the literature of upward vertical two-phase flow. The views

of the previous researchers from different schools of thought have been discussed and some controversial observations have been presented in Chapter II. Subsequently, Chapter III discusses the system of design, means of construction, and the experimental procedure executed. Chapter IV presents the results of the experiments obtained from the photographic and visual observations of flow patterns and from the measurements of void fraction of the gas-liquid flow and pressure drop along the test section. Finally, conclusions of this work and recommendations for future work have been presented in Chapter V.

CHAPTER II

PREVIOUS WORK IN GAS-LIQUID TWO-PHASE FLOW

This chapter analyzes the technological developments in the gas-liquid two-phase flow studies with a historical perspective. A systematic review of two-phase systems is highly time-consuming because of the voluminous literature available on this subject. Nevertheless, an assiduous survey was performed to elucidate the two-phase flow mechanisms.

Historical Perspective

Gas-liquid two-phase flow has a rich literature and has gained considerable importance in recent years. A good deal of research on this phenomenon is being carried out at several institutions all over the world. The Atomic Energy Research Establishment at Harwell, England, and several universities in the United States are involved in gas-liquid two-phase flow studies. Most investigators are interested in the hydrodynamics of two-phase flow which would aid the description of heat and mass transfer mechanisms in a system. Although most of the important work on two-phase flow was done in connection with the design of nuclear reactors, this type of flow plays a very important role in the chemical process industries as well. The oil and gas industries have been doing extensive investigation on the two-phase flow phenomenon in their wells. Therefore, the significance of two-phase flow need hardly be overemphasized.

Two-phase phenomenon has been reported (Chisholm, 1983) to have been observed as early as in the seventeenth century. Compressed air was generated for use in iron and brass smelting by an arrangement shown in Figure 1. Early design models (until the 1940s) relied on the homogeneous flow approach, which assumes equal velocities for both the fluid phases, for calculating the density of the two-phase mixture. This homogeneous density was then used to calculate the frictional pressure gradient due to the two-phase flow as it would be done for a single phase flow. The homogeneous theory has been reported (Chisholm, 1983) to work well in certain cases such as in well-designed boilers. It, however, has been shown to give gross errors in most cases, by as much as a factor of three to four, either due to underprediction or overestimation of the pressure loss depending on the geometry of the conduit. Practically, there would hardly be a case found where the velocities of the two phases are equal as assumed by the homogeneous theory.

General Definitions

One of the earliest studies to evaluate the homogeneous theory was done by Moore and Wilde (1931) as discussed by Chisholm (1983). They used quick-closing cocks at both ends of a vertical pipe to trap the two phase fluid and measure the fractions of the two phases in the mixture. Subsequently, this technique was used by many experimenters including Galegar et al. (1954), Govier et al. (1957), Fernandes et al. (1983) and Mao et al. (1993) to measure the holdup in the flow. A similar approach, using solenoid valves as quick-closing valves, was adapted in this work to measure the holdup for calculating the void fraction of the flow. It was found that the gas phase volume fraction in the holdup was not equal to that calculated using the superficial volumetric flow rates of the two fluids. This implies a relative motion between the two fluids which contradicts the basic assumption in the homogeneous flow approach. Bell (1993) attributes the slippage to the relatively high density and viscosity of the liquid
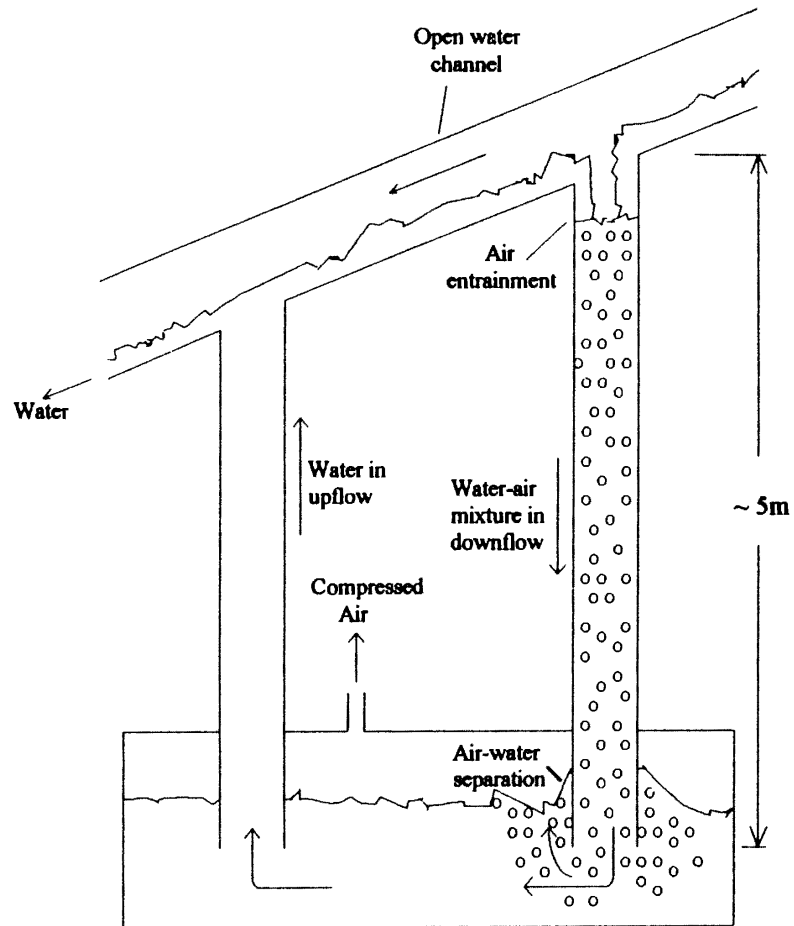
Figure 1.   Apparatus for the Generation of Compressed Air.
[Adapted from Chisholm (1983)].

phase relative to those of the gas phase. The volume fraction of the gas phase in the holdup was termed as the void fraction, R_v, and was defined as the "in-situ" volume fraction of the gas phase in the two-phase mixture. The liquid phase volume fraction, R_l, was observed to be $(1-R_v)$.

Another way of representing the fractions of the two fluids is on a mass basis. The quality, x, is defined as the mass fraction of the gas phase in the two phase mixture and is given by

$$x = \frac{\dot{m}_g}{\dot{m}_g + \dot{m}_l} = \frac{\dot{m}_g}{\dot{m}_T}. \tag{1}$$

The relative motion between the liquid and the gas was termed as slip and was quantified as slip ratio, s_r, given by

$$s_r = \frac{v_g}{v_l}, \tag{2}$$

and as slip velocity, s_v, given by

$$s_v = v_g - v_l. \tag{3}$$

Bell (1993) also suggests that the slip ratio is usually greater than 1 and can reach 20 or larger. The relation between the slip ratio and the fractions of the fluids in the two-phase mixture is given by

$$s_r = \frac{v_g}{v_l} = \left(\frac{\rho_l}{\rho_g}\right)\left(\frac{1-R_v}{R_v}\right)\left(\frac{x}{1-x}\right). \tag{4}$$

The major contributions to the total pressure gradient during an adiabatic two-phase flow are the frictional and hydrostatic effects. The equations used to calculate these effects are discussed in Chapter III. Martinelli et al. (1944) were the first to build a systematic basis for correlating two-phase frictional pressure drops. They developed an equation which used a multiplier to relate the actual pressure drop of the two-phase flow to the pressure drop when only a single phase fluid was flowing in the tube. The equations developed by Martinelli et al. (1944) are being used by many workers for estimating the

frictional pressure gradient during two-phase flow and are discussed in Chapter III. This work has used these correlations for design and verification of the results.

Flow Regime Analysis

The description of two-phase flow in conduits is highly intricate due to the existence of an interface between the two phases. For gas-liquid two-phase flow, this interface exists in a variety of forms depending on the flow rates and phase properties of the fluids, and also on the inclination and geometry of the tube. The complexity of the interface indicates that the modeling of a two-phase flow would be extremely cumbersome and error-bound if constraints are not introduced to describe the flow configuration or the geometry of the various interfacial structures. Therefore, the concept of flow patterns or flow regimes was introduced. The characteristic distribution of the two phases in the conduit was conveniently classified using this concept.

There has been substantial discordance in the description of visual observation of two-phase flow provided by different investigators. Some of the prevalent terms used to describe the various flow patterns are bubbly, dispersed bubbly, piston, slug, frothy, churn, ripple, annular, mist, wispy annular, etc. Although the chaotic nature of two-phase flow makes it difficult to classify the flow regimes and assign transition criteria to them, there has been good agreement among the investigators in the acceptance of the major flow regimes for an upward cocurrent gas-liquid two-phase flow in a vertical tube. For the purpose of this work, the major flow regimes, namely, the bubbly, slug, churn and annular flow regimes, were considered. The controversial churn flow regime will be discussed in detail later in this chapter. The other terms indicated above could be considered as subdivisions of the major flow regimes under consideration, or as those that describe flow structures in proximity to the regime transitions.

Classification of flow structures into definite flow regimes is essential for efficient modeling of two-phase systems. In order to classify the flow patterns, the regime transitions have to be thoroughly studied. Bubbly, slug and annular flows have been unanimously accepted as major flow regimes of upward vertical gas-liquid flow. On the other hand, the existence and behavior of the churn flow regime have always been in debate in the past. To unravel the problem, a review of the definitions of the major flow patterns and the mechanisms of flow regime transitions have been performed, and the following section has been devoted to this discussion.

When the gas phase tends to rise through a liquid continuum as small, discrete bubbles, usually as distorted spheres, the regime is called bubbly flow. At higher bubble concentrations, bubble coalescence occurs and large bullet-shaped bubbles with a nearly spherical nose and a flat tail are formed. These bubbles are called Taylor bubbles and their radial size is of the same order of magnitude as the tube diameter. Two successive Taylor bubbles are bridged by liquid slugs which may or may not contain a dispersion of smaller gas bubbles. This type of flow is called slug flow. If the gas flow rate is further increased, the slug flow structure gradually becomes unstable. This instability eventually results in the complete destruction of the slugs with consequential oscillatory action or churning. This is called the churn flow regime. At very high gas flow rates, the liquid flows as a uniform annular film on the tube wall while the gas flows as a central core inside the liquid annulus. This pattern is referred to as the annular flow regime.

Schematic diagrams of the major flow regimes are presented in Figure 2. The diagrams give a clear perspective of the flow patterns due to the various gas-liquid distributions.

Flow

BUBBLY   SLUG   CHURN   ANNULAR
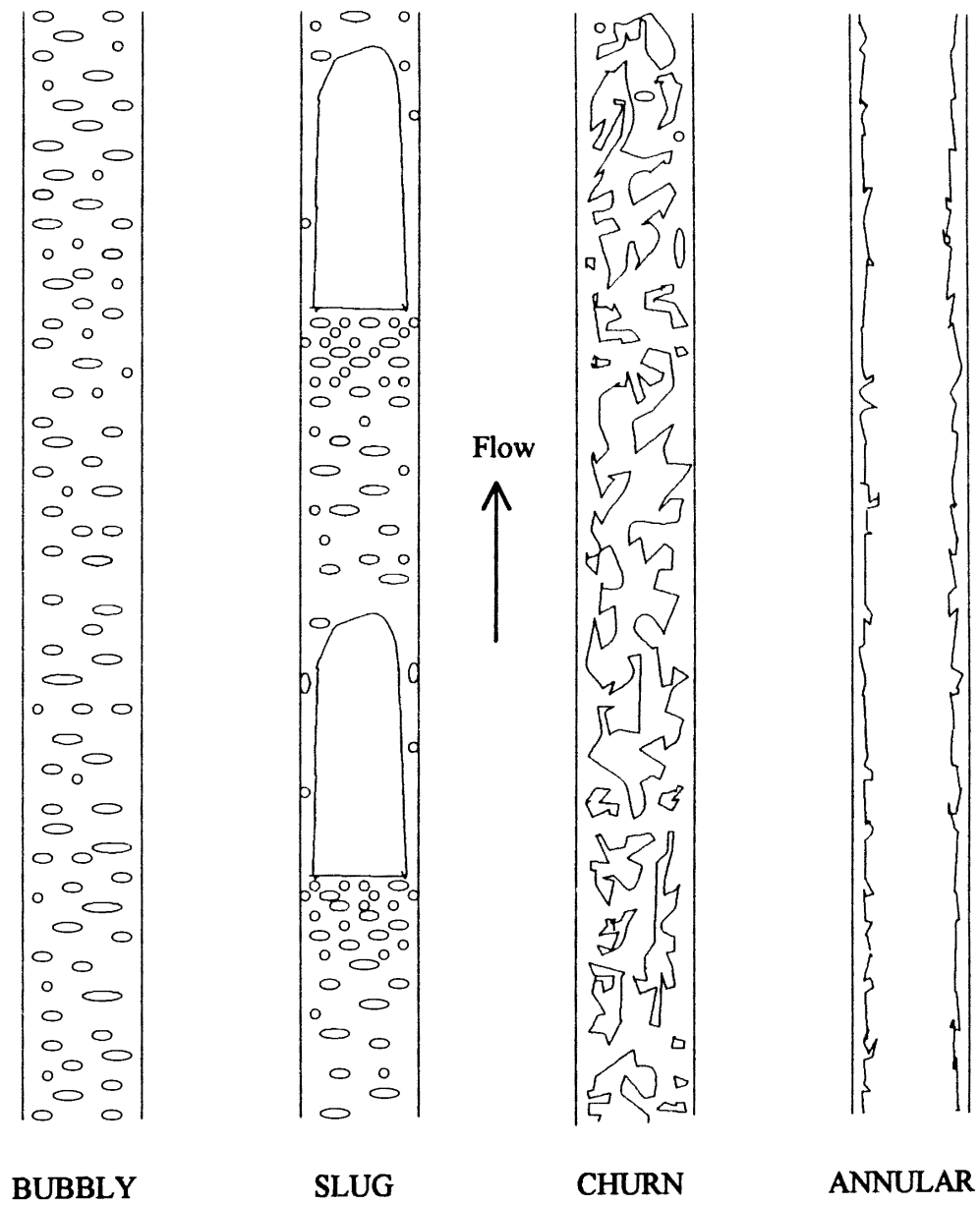
Figure 2.   Schematic Diagram of the Major Flow Patterns of Vertical Gas-Liquid
Two-phase Flow.

Bubbly Flow

This regime is the easiest to imagine from day-to-day experience. Bubbly flow can easily be generated either by injection of the gas phase into a liquid column or by a falling liquid film that would entrain small amounts of gas into the liquid (Rhodes, 1982). The volumetric flow rate of the gas, however, has to be minimal in order to keep the bubbles as discrete entities. If the gas flow rate is increased, bubbles collide and eventually result in the formation of Taylor bubbles and hence in the transition from bubbly to slug flow regime.

Bubbly-Slug Transition

Bilicki et al. (1987) have explained the bubbly-slug transition considering that, at some places in the flow field, one bubble follows another and accelerates into the wake of the former which creates a tendency for the bubbles to collide and coalesce. The authors have also assumed that the transition occurs when the ensemble averages of the actual distance between the two bubbles and the characteristic length (the length between the bubbles above which they cease to interact) become equal. They have concluded that the transition was not sharp, as the above mentioned lengths were highly stochastic in nature.

McQuillan et al. (1985) have illustrated a model developed by Taitel et al. (1980) to explain the transition. They have considered two controlling processes for the stability of bubble flow. They are those of bubble coalescence caused by collisions and bubble breakup caused by pressure forces resulting from turbulence in the liquid phase.

Slug Flow

Fernandes et al. (1983) developed a hydrodynamic model for this flow pattern. In their analysis, they reported that, as the liquid is shed from the back of a slug to form a falling film around the Taylor bubble, it is essentially free from the small bubbles seen in the liquid slug. They attributed the bubble-free film to the larger diameter of the distributed bubbles in the slug with respect to the thickness of the falling liquid film. This argument has been contradicted by the results of the present work and will be discussed in Chapter V.

Slug-Churn Transition

Jayanti et al. (1992) have discussed four mechanisms for the transition from the slug to churn flow. They are (1) the entrance effect mechanism, (2) the flooding mechanism, (3) the effect of wake formation, and (4) the bubble coalescence mechanism.

Jayanti et al. (1992) have illustrated the entrance effect mechanism using the treatment of churn flow by Dukler and Taitel (1986) as an entrance phenomenon. Jayanti et al. (1992) have presented a formula,

$$\frac{l_e}{D} = 42.6\left(\frac{U_m}{\sqrt{gD}} + 0.29\right), \tag{5}$$

derived by Dukler and Taitel (1986) to evaluate the entrance length, l_e, required to form stable slugs in a given flow situation. Dukler et al. (1986) concluded that if the actual tube length is less than the entrance length calculated using the above formula, churn flow may be observed.

The second mechanism discussed by Jayanti et al. (1992) involves flooding as a mechanism of slug-churn transition. They cite a number of researchers (Nicklin and Davidson, 1962; McQuillan and Whalley, 1985; Govan et al., 1991) for their work on this mechanism. Flooding is a phenomenon in which the liquid film during a countercurrent flow of gas and liquid breaks down due to the formation of large interfacial waves. Jayanti et al. (1992) indicate that a link between flooding and churn flow has been established experimentally by Wallis (1961) and Chaudhry et al. (1965).

As a third possibility, Jayanti et al. (1992) have described the wake effect of the Taylor bubbles as the mechanism of transition. Mishima et al. (1984) have explained that, as the gas rate increases during the slug flow, the Taylor bubbles gradually become longer and the liquid slugs become shorter. The proximity of the Taylor bubbles would create a strong wake effect which would destabilize the liquid slug and destroy it.
Mishima et al. (1984) also state that the transition occurs when the void fraction in the pipe is just greater than the mean void fraction over the Taylor bubble region.

Finally, Jayanti et al. (1992) have presented the phenomenon of slug collapse by bubble coalescence as another mechanism found in the literature for the slug-churn transition. Brauner and Barnea (1986) have attributed the transition to the formation of highly aerated liquid slugs. They state that the transition occurs when the void fraction in the liquid slug is greater than 0.52.

Jayanti et al. (1992) have used experimental results to comment on the efficacy of the four models discussed above. They have discovered that the flooding model of McQuillan and Whalley (1985) and the excessive bubble entrainment model of Brauner and Barnea (1986) show good agreement with experimental results, although in a limited range at low and high liquid flow rates, respectively. They have tried to improve the flooding model of McQuillan and Whalley (1985) by overcoming two shortcomings in the model. They have replaced the Nusselt equation for the laminar flow of the falling film with an empirical correlation of Brotz (1954) that had been found to be applicable over a

wide range of film Reynolds numbers (Fulford, 1964). Jayanti et al. (1992) have also pointed out that the second shortcoming of the McQuillan-Whalley model was the neglect of the length effect of the falling film on the flooding velocity. Jayanti et al. (1992) illustrated the length effect using Figure 3 (from Jayanti et al., 1992) which shows the variation of the flooding gas flow rate as a function of the liquid flow rate for different lengths of the counter-current flow test sections having similar inlet and outlet configurations. From Figure 3, it can be observed that the flooding velocity increases with a decrease in the length of the test section and hence the length of the falling liquid film. Jayanti et al. (1992) developed a new equation, taking the length effect into account, and found that it gave much improved predictions. They concluded that the flooding mechanism was capable of predicting the slug to churn flow transition over the full range of liquid flow rates. They also added that more direct evidence would be required to establish the likelihood of the flooding mechanism as the cause for the transition.

Hewitt et al. (1993) provided direct evidence for the description of the transition in terms of the formation of flooding waves. They have recorded the flooding event on video and reported that it was a visual confirmation of the transition in terms of flooding. They have explained the sequence of events that lead to fully developed churn flow. Following flooding there is a reduction in the amount of liquid fed down the Taylor bubble and into the succeeding slug while the slug is draining into the next Taylor bubble at a rate which is substantially unaffected by the flooding process. The slugs would eventually collapse and liquid transport would take place by the large flooding waves. These waves, which are sometimes large enough to partially block the tube, are associated with high liquid entrainment rates. Another characteristic of the churn flow regime is the enhanced bubble entrainment rate into the liquid in the waves in the residual slugs which could be a cause for the collapse of the slugs (Hewitt et al., 1993).

The flooding phenomenon has been defined by France et al. (1989) as a transition from countercurrent to cocurrent flow. This is exactly what happens when the downward
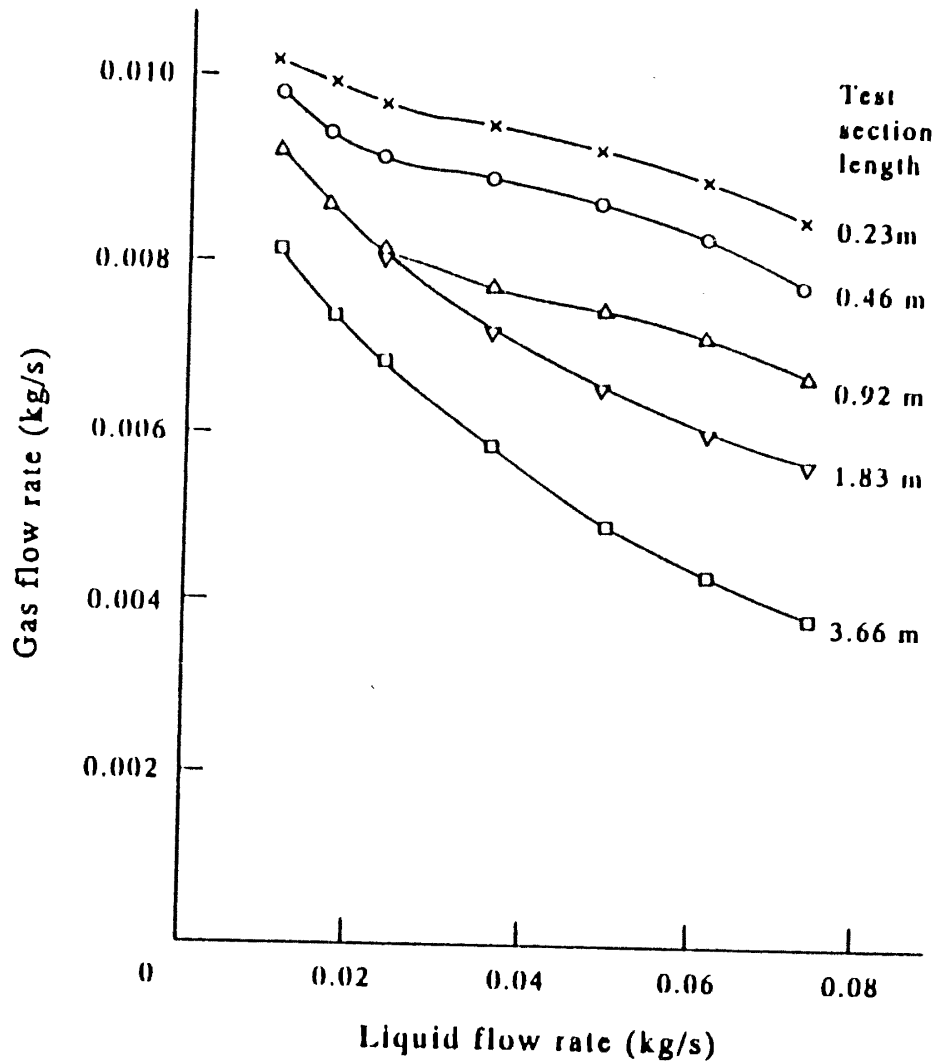
Figure 3. Variation of the Flooding Gas Flow Rate as a Function of the Liquid Flow Rate for Different Lengths of a Counter-current Flow Test Section [From Jayanti et al. (1992)].

motion of the falling film around the Taylor bubble changes direction and flows upward after the slug-churn transition is complete.

In summary, the flooding mechanism seems to be best of all the mechanisms in describing the transition from the slug to churn flow.

Churn Flow

Occurrence of churn flow normally lies between the slug and annular flows in terms of the gas flow rate, at a constant liquid flow rate. However, there could be a direct transition either from the slug or bubbly flow to the annular flow at very high liquid flow rates. Identification of this pattern has been reported by many investigators, including Taitel et al. (1980) and Mishima et al. (1984), based on visual observations and conductance probe analyses. These investigators are only a few among those who have tried to model the transition from the slug to churn pattern.

Mao et al. (1993) suggest that there is little justification for considering churn flow as a distinct flow regime and that churning is just a simple and continuous extension of the slug flow condition. They argue that visual observation could be notoriously deceptive due to the presence of multiple interfaces which scatter transmitted and reflected light in complex ways creating false visual images. They conclude that churn flow is apparently a manifestation of slug flow and that it could be modeled using slug flow analysis.

Hewitt et al. (1993) have responded to the description of churn flow by Mao and Dukler (1993). They describe the unique features of churn flow as the formation of flooding waves that persist throughout the regime and the flow reversal in the film region near the wall.

The intent of defining a flow regime is to develop a model for each flow regime. A better prediction of two-phase flow variables could be accomplished by using a different model for each flow regime. As churn flow stands out from the other flow patterns,

chiefly due to its periodic flow reversal and enhanced entrainment capabilities, it has to be considered as a separate flow regime for improved predictions. This perspective is consistent with that of Hewitt et al. (1993) who have presented arguments for considering churn flow as a distinct flow pattern.

Churn-Annular Transition

Taitel et al. (1980) have reported that the annular flow occurs when the gas flow rate becomes high enough to lift the entrained liquid droplets. They have balanced the drag and gravity forces acting on a droplet to arrive at an equation for the minimum gas velocity required to suspend a droplet as

$$v_{gs} = 3.1 \frac{[\sigma g(\rho_l - \rho_g)]^{1/4}}{\rho_g^{1/2}}. \tag{6}$$

Taitel et al. (1980) obtained the value 3.1 in equation (6) by using the units of m/s for the superficial gas velocity, m/s^2 for the acceleration due to gravity, N/m for the surface tension and kg/m^3 for the densities of two fluids. They conclude that the transition to annular flow regime takes place when the actual superficial gas velocity exceeds the value of v_{gs} calculated using equation (6).

McQuillan and Whalley (1985) indicate that the equation derived by Taitel et al. (1980) has a similar form as the one presented by Pushkina and Sorokin (1969) for predicting flooding of a falling liquid film. They themselves have presented an inequality,

$$v_{gs}^* \geq 1, \tag{7}$$

as a criterion for the existence of annular flow where v_{gs}^* is a modified Froude number that represents a comparison between the inertial and gravity forces. They have used the critical value of unity which had been experimentally verified for the air-water system by

Hewitt and Wallis (1963). This inequality has been shown by McQuillan and Whalley (1985) to have produced better results than that obtained from the equation presented by Taitel et al. (1980).

Bilicki and Kestin (1987) tried to determine the conditions under which the film thickness could be sustained in its upward flow by the shear stress produced by the gas stream which slips past the liquid film. They arrived at an equation for v_g from the definition of the Kutateladze number given by

$$Ku = \frac{v_g \cdot \rho_g^{1/2}}{[g\sigma(\rho_l - \rho_g)]^{1/4}},$$ (8)

$$as \quad v_g = \frac{Ku[g\sigma(\rho_l - \rho_g)]^{1/4}}{\rho_g^{1/2}},$$ (9)

through a dimensional analysis. The Kutateladze number presents a balance between the inertial forces in the gas, the buoyancy and surface tension forces.

It could be observed that equation (9) is also very similar to the one derived by Taitel et al. (1980). Bilicki and Kestin (1987) have reported a value of Ku = 3.2 below which frothing or churning would occur.

Annular Flow

A characteristic feature of gas-liquid annular flow is that the gas flows in the core region of the conduit dragging the liquid along the walls of the tube as an annulus. As the gas-liquid interface governs almost all associated variables, studies have been performed by many investigators on the interfacial waves that exist during an annular flow. Hewitt (1969) has indicated that the waves could be of considerable amplitude and that liquid entrainment from the wave tips is a common and important phenomenon.

Hall-Taylor et al. (1963) categorize the regions of annular flow as non-wetting region, ripple wave region, disturbance wave region, and the pulse region. Other researchers who have been involved in studies pertaining to waves in annular flow conform to the major classification of the annular flow regime as ripple and disturbance wave regions.

A clear distinction between the major regions of annular flow has been provided by Hall-Taylor et al. (1968). They reported that the ripples have a wavelength of a few millimeters and that they form and disappear while they travel. On the other hand, the disturbance waves are spaced at about 4 to 12 inches apart and retain their identity throughout their travel. They also state that the ripples traverse at a much lower velocity than the mean liquid velocity with an amplitude less than the mean film thickness, while the disturbance waves propagate at a velocity of the same order of magnitude as the mean liquid velocity with an amplitude much higher than the film thickness. Hewitt (1969) presents a possible magnitude for the amplitude of the disturbance waves as five times as much as the mean film thickness, or even greater. A clear cut transition between the two waves has been reported by Nedderman et al. (1963).

One of the best means of visual observation of annular flow has been the high-speed axial-view photography (Hewitt, 1969). A study using this technique has shown (Rhodes, 1982) that the droplets are released explosively from the waves. From his wave studies, Hewitt (1969) concluded that the ratio between mean wave amplitude and mean film thickness is approximately constant, independent of the flow conditions. This conclusion agreed perfectly with the observation, by the same author, that the effective interfacial roughness for a given value of mean film thickness is constant. The above discussion clearly indicates the importance of studies on interfacial waves for a better understanding the nature of vertical annular flow.

Many articles have been published on various aspects of two-phase flow, but much work is still required to solve many problems. The major limitation of all the experimental

work done in two-phase flow, including this work, is the unavailability of data covering the whole range of two-phase flow conditions. Modeling of flow regime transitions is one way of partially overcoming this problem. In order to do this, the mechanisms involved need to be studied in detail.

CHAPTER III

DESIGN, CONSTRUCTION, AND EXPERIMENTAL PROCEDURE

The main objective of this work was to develop equipment to study the gas-liquid two-phase phenomenon accompanied by its exotic flow patterns. A safe, economic, and flexible design was developed with the help of the literature available on gas-liquid two-phase flow. Safety and space optimization were considered during the construction of the equipment. Experiments were performed to determine the important variables, such as the void fraction of the flow and the pressure drop, for the description of two-phase flow.

The three major stages of the development of this equipment, the design, the construction and the experimental procedure, are discussed in detail in this chapter.

Design Methods

The principal goal, at this stage, was to calculate flow rates of air and water required for the observation of all the flow regimes of upward gas-liquid two-phase flow and to get an estimation of the void fraction and pressure drop of the two-phase mixture.

Determination of Pipe Size

The calculation of the flow rates is required for estimating the pipe size for which all the flow patterns could be observed. To assure that the required flow rates are obtainable with the equipment, the flow regime map developed by Fair (1960) was used.

The map, shown in Figure 4 (adapted from Bell, 1993), is a plot of a Martinelli parameter, X_{tt}, given by

$$X_{tt} = \left(\frac{1-x}{x}\right)^{0.9} \left(\frac{\rho_g}{\rho_l}\right)^{0.5} \left(\frac{\mu_l}{\mu_g}\right)^{0.1},$$

(10)

versus the total mass velocity, G_T, given by

$$G_T = \frac{\dot{m}_g + \dot{m}_l}{S} = \frac{\dot{m}_T}{S}.$$

(11)

The subscript 'tt' of the Martinelli parameter, X_{tt}, indicates that turbulence in both the fluids is involved in the two-phase flow. Another of the several Martinelli parameters used in this work is χ_{tt}, given by

$$\chi_{tt} = \left(\frac{1-x}{x}\right) \left(\frac{\rho_g}{\rho_l}\right)^{0.57} \left(\frac{\mu_l}{\mu_g}\right)^{0.11}.$$

(12)

It can be observed that

$$X_{tt} \cong \chi_{tt}^{0.9}.$$

(13)

Martinelli et al. (1944) used these parameters to correlate the experimental data for different fluids and tube geometries. The ordinate of the map, shown in Figure 4, is dimensional and hence the units given in the figure were used. The abscissa of the map is dimensionless and therefore a consistent set of units was used. Various tube sizes and total mass velocities were considered and a 1 inch internal tube diameter was found to be the most suitable size for the available supply of air and water. The physical properties of the fluids used as well as the geometrical data have been provided in Appendix A.
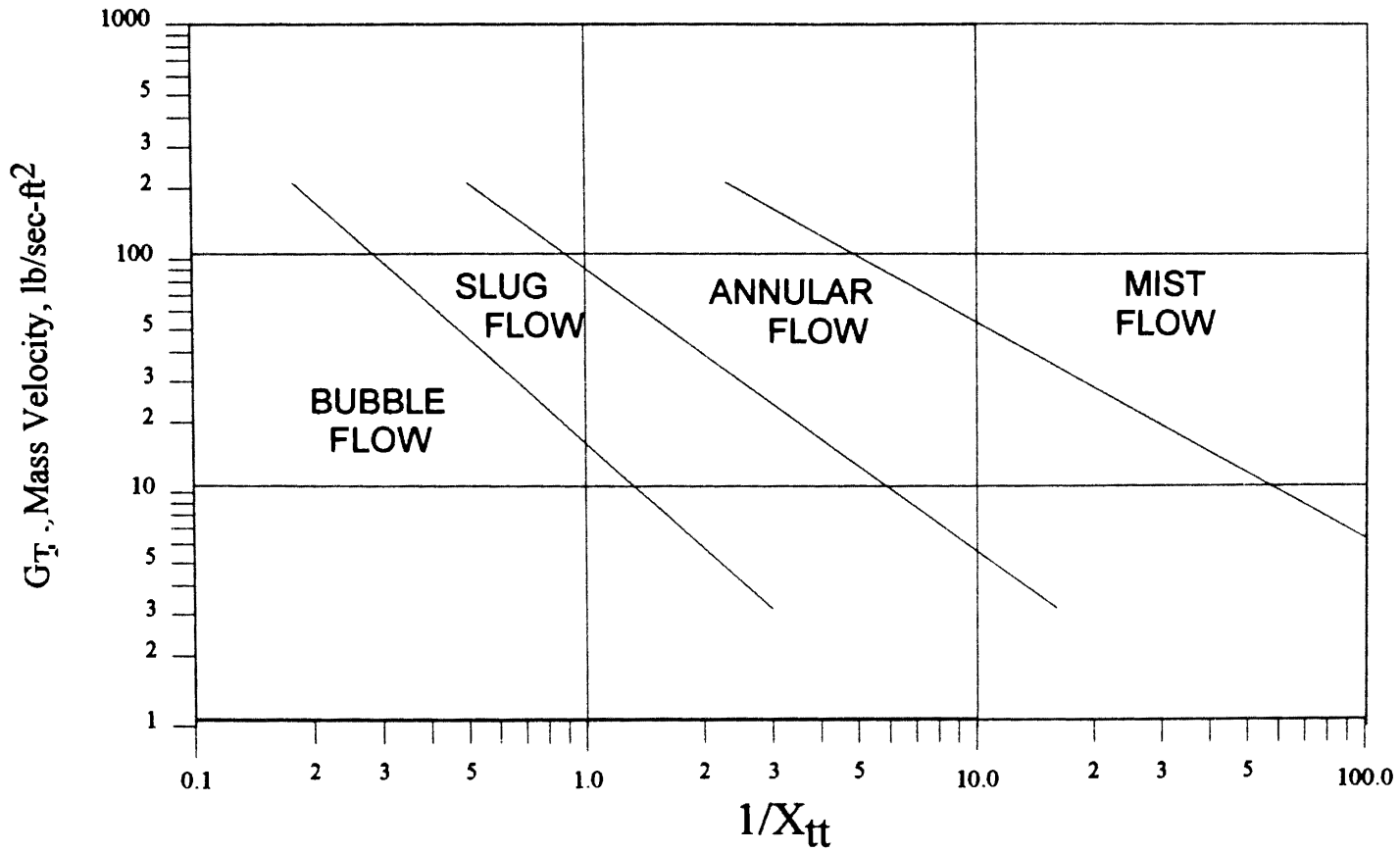
Figure 4. Flow Regime Map Developed by Fair (1960) for Vertical Intube Two-phase Flow.

Void Fraction Estimation

An estimation of the void fraction of the flow is required primarily for the estimation of the hydrostatic effect on the total pressure drop during the flow. Martinelli and Nelson (1948) developed a graph between the "in-situ" volume fractions of the two fluids, R_v and R_l, and $\sqrt{\chi_{tt}}$ for various values of the fluid pressures. The modified graph presented by Bell (1993) is shown in Figure 5, and was used in obtaining an estimation of the void fraction of the flow.

Pressure Gradient Estimation

The total pressure drop in a section of pipe can be considered to arise from three separate sources. The three major contributions for the total pressure drop during two-phase flow are:

Friction. In addition to the frictional loss due to the surface roughness of the conduit that is normally prevalent even during single phase flow, two-phase flow also encounters pressure loss due to the roughness of the gas-liquid interface. An estimate of the magnitude of the pressure loss due to the frictional effect was calculated using the correlation developed by Martinelli et al. (1948). The basic procedure as given by Bell (1993) is described below:

The pressure drop was calculated, considering a single phase liquid flow in the column, using

$$\left(\frac{dP}{dl}\right)_{f,l} = -\frac{2f_l G_l^2}{g_c \rho_l D_i}. \tag{14}$$

The Reynolds number of the liquid phase was found using
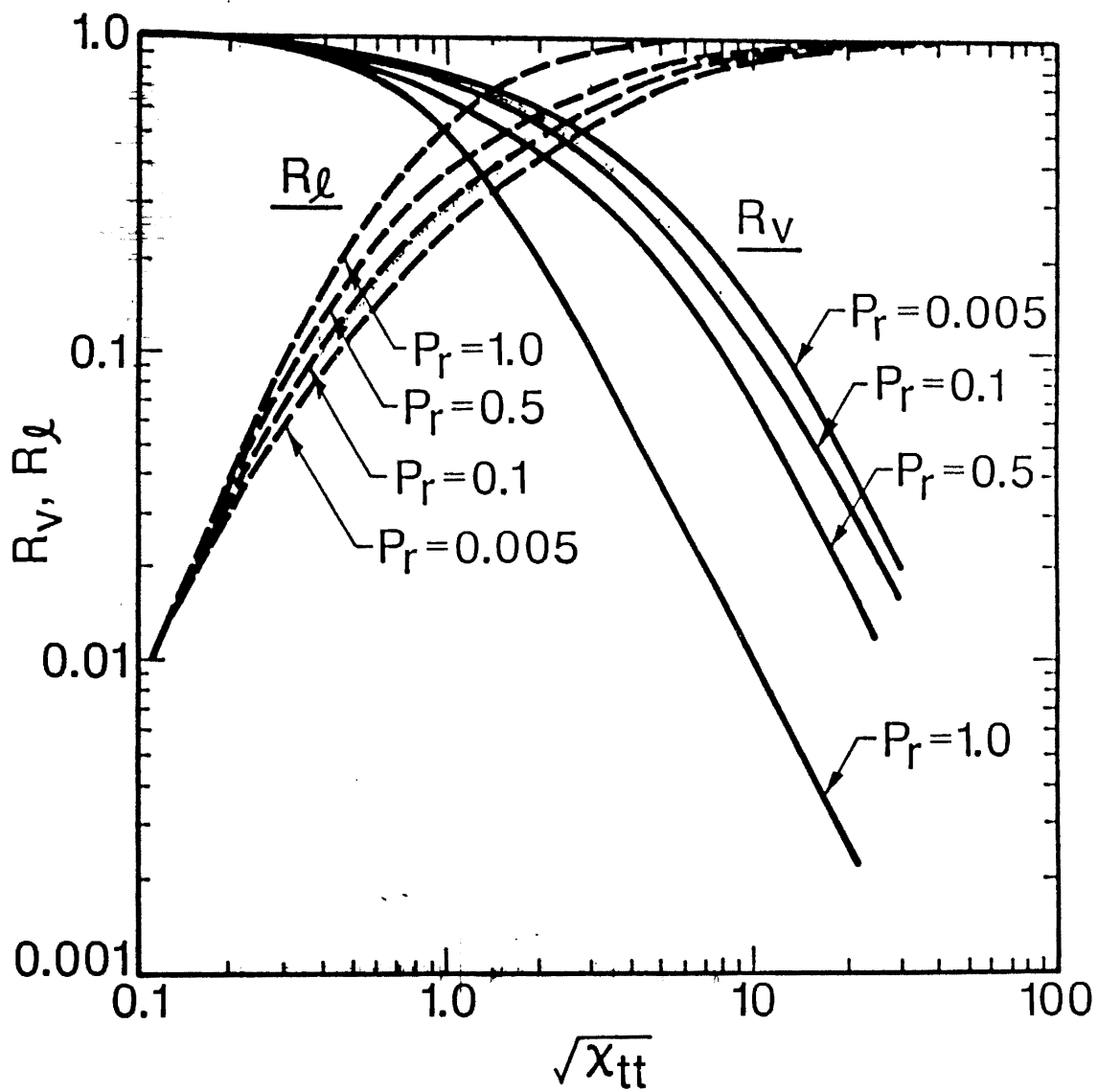
Figure 5.   Modified Graph for a Relation Between the Volume Fractions
of the Fluids and $\sqrt{\chi_{tt}}$ [From Bell (1993)].

$$Re_l = \frac{D_i G_l}{\mu_l}. \tag{15}$$

Only the method valid for $Re_l > 2100$ is discussed here as the experimental conditions of this work were such that Re_l was always much greater than 2100. Bell (1993) also describes a method applicable to $Re_l < 2100$, which will not be included in this discussion. The friction factor was obtained from the equation,

$$f_l = \frac{0.079}{(Re_l)^{1/4}}. \tag{16}$$

The pressure loss, due to friction, for the two-phase flow was then obtained from,

$$\left(\frac{dP}{dl}\right)_{f,TPF} = \Phi_{lu}^2 \left(\frac{dP}{dl}\right)_{f,l}, \tag{17}$$

where Φ_{lu} is a multiplication factor that relates the pressure loss due to the two-phase flow to the pressure loss considering only a single phase liquid flow. The value of Φ_{lu} was read from Figure 6 (from Bell, 1993) at the appropriate value of $\sqrt{\chi_{u}}$.

Kinetic Energy Changes. Momentum effects due to the change in kinetic energy of the stream make little contribution to the total pressure drop for the case under consideration. This conclusion is derived from the fact that there is little change in the velocity of a fluid during an adiabatic flow. Zero solubility of air in water, and negligible expansion of the gas phase have also been assumed.

Hydrostatic Effect. This term arises whenever there is a change in elevation of the fluid. Due to this effect, the pressure of the fluid decreases in an upward direction. For a vertical upward flow, the pressure loss due to this effect is usually the most dominant of all the contributors, especially in cases of high liquid fraction in the two-phase fluid. The density of the mixture is an essential parameter for the calculation of the hydrostatic head. The effective density of the two-phase mixture, ρ_{eff}, is given by
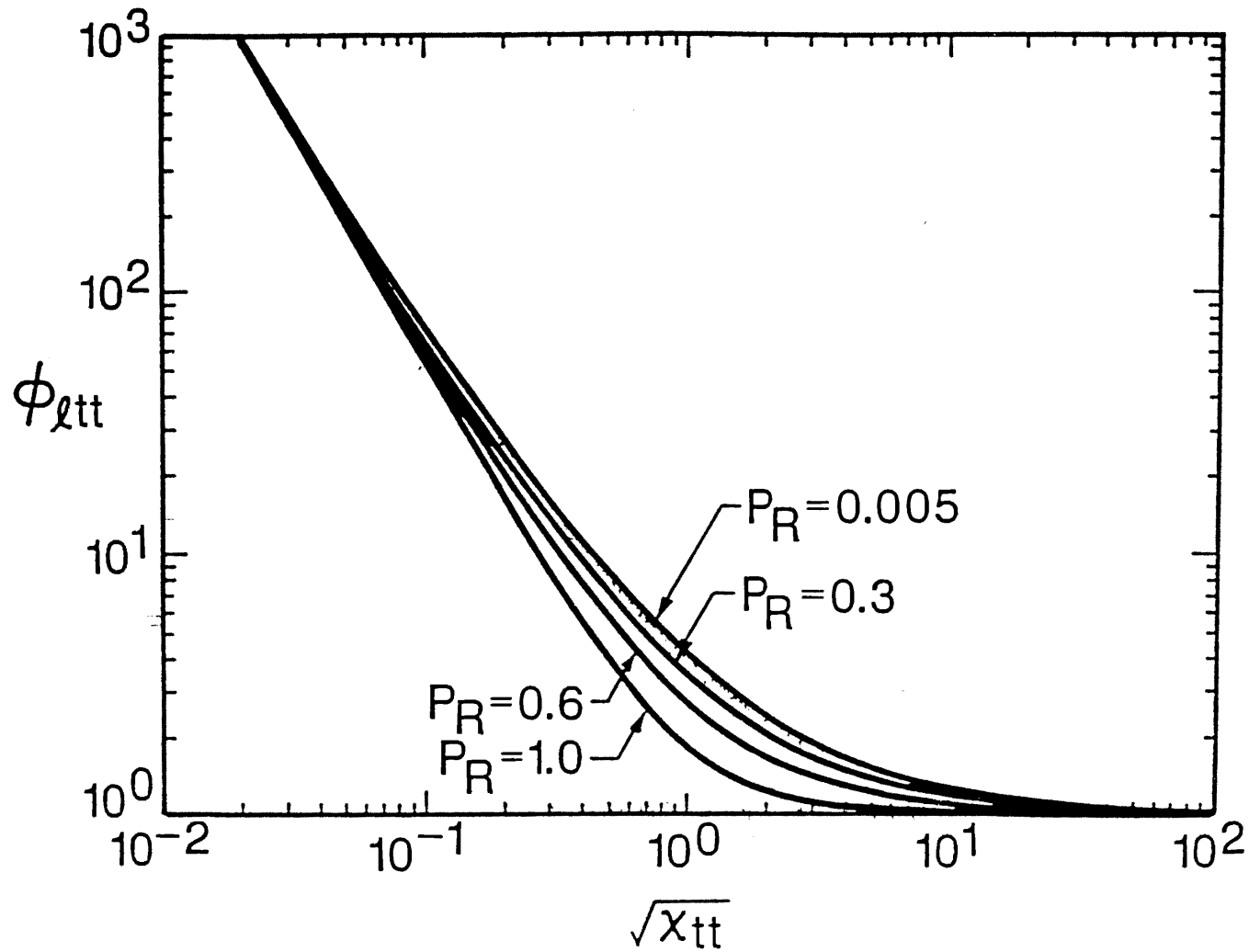
Figure 6. Relation Between $\sqrt{\chi_{tt}}$ and the Multiplier Φ_{ltt} [From Bell (1993)].

$$\rho_{\text{eff}} = \rho_g R_v + \rho_l (1 - R_v).$$ (18)

The pressure gradient due to the hydrostatic effect was calculated from,

$$\left(\frac{dP}{dl}\right)_{g,TPF} = \rho_{\text{eff}} \frac{g}{g_c} \cos\theta,$$ (19)

where θ is the angle of inclination of the tube from the vertical. For a vertical conduit, $\theta = 0$ and hence $\cos\theta = 1$. Therefore,

$$\left(\frac{dP}{dl}\right)_{g,TPF} = \rho_{\text{eff}} \frac{g}{g_c}.$$ (20)

Assuming that the pressure loss due to momentum effects is zero, the total pressure drop is the algebraic sum of the frictional loss and the loss due to hydrostatic effects. This can be mathematically represented as

$$\left(\frac{dP}{dl}\right)_{T,TPF} = \left(\frac{dP}{dl}\right)_{f,TPF} + \left(\frac{dP}{dl}\right)_{g,TPF}.$$ (21)

Construction

A safe, compact and convenient apparatus was designed with economical concerns. Most of the pipelines were constructed using 1 inch internal diameter PVC pipes. A transparent PVC pipe was used as the test section in order to permit visual observation. The transparent test section is of 1.029 inch internal diameter and 0.14 inch wall thickness. The total height of the clear tube is 15 feet.

A schematic diagram of the experimental apparatus is shown in Figure 7. As the diagram is two-dimensional, the actual experimental structure is not geometrically the same as it appears in the diagram. However, the order in which the components are placed in the diagram is similar to that in the experimental setup. A photograph of the
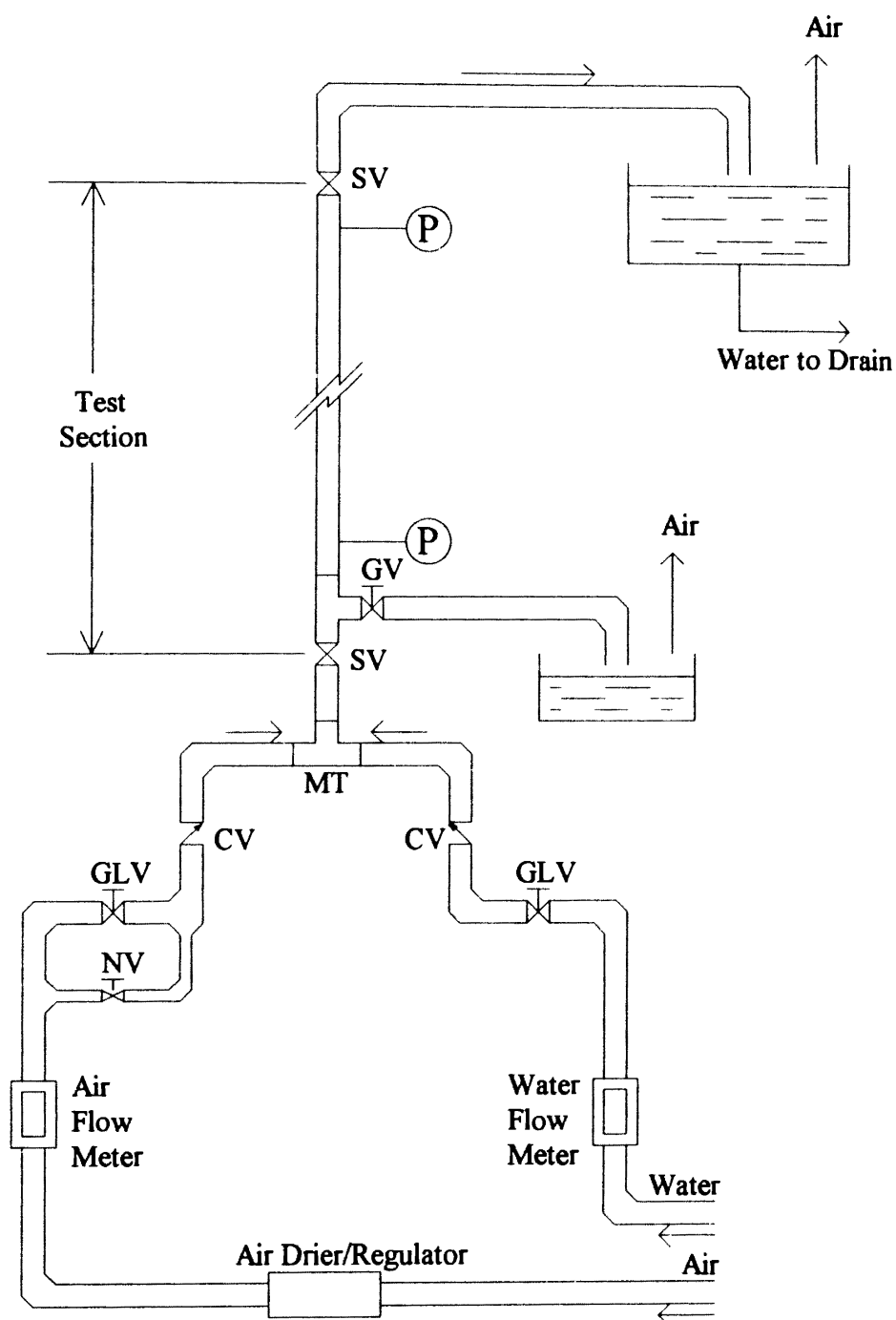
GLV - Globe Valve   CV - Check Valve
SV - Solenoid Valve   MT - Mixing Tee
Height of Test Section (Between the Pressure Taps) = 15.8 ft

Figure 7.   Schematic Diagram of the Experimental Apparatus.

front view of the arrangement is presented in Figure 8. Both water and air inlets are provided with ball valves (not in the diagram) for isolation of the streams. The air stream enters through an air drier/regulator where the moisture content in air is removed and the air pressure adjusted. Both air and water streams are provided with rotameters (ranging 3-25 SCFM and 0.4-5 gpm respectively) to measure the rate of flow, globe valves to regulate the flow, and check valves to maintain unidirectional flow. In the air stream, a needle valve is included in parallel to the globe valve to obtain low flow rates of air for the observation of the bubbly flow pattern. A mixing tee is provided where the two streams come in contact, mix and flow upwards.

Two solenoid valves, as shown in the Figure 7, act as the quick-closing valves at both ends of the test section. A switch is used to operate both the valves simultaneously. An outlet with a gate valve is provided at the bottom end of the test section in order to allow measurements of the amounts of the two fluids in the holdup. At the downstream end of the pipeline, the two fluids are separated in a plastic container. If valuable, flammable or toxic fluids were used for the study, the fluids could be recirculated by using a closed separator.

Two pressure transducers are installed to measure the pressure drop between the top and bottom of the test section. The signals from these sensors are transmitted to a signal conditioner that acts as a subtraction module. This module essentially subtracts one pressure from the other and sends the difference to the digital readout. Therefore, the pressure drop due to the flow along the test section is read directly from the display. The circuit diagram, given in Figure 9, describes the related electrical connections.

Experimental Procedure

The different flow patterns were observed by varying the flow rates of the two feed fluids. Visual observation and photographic techniques were used to study the
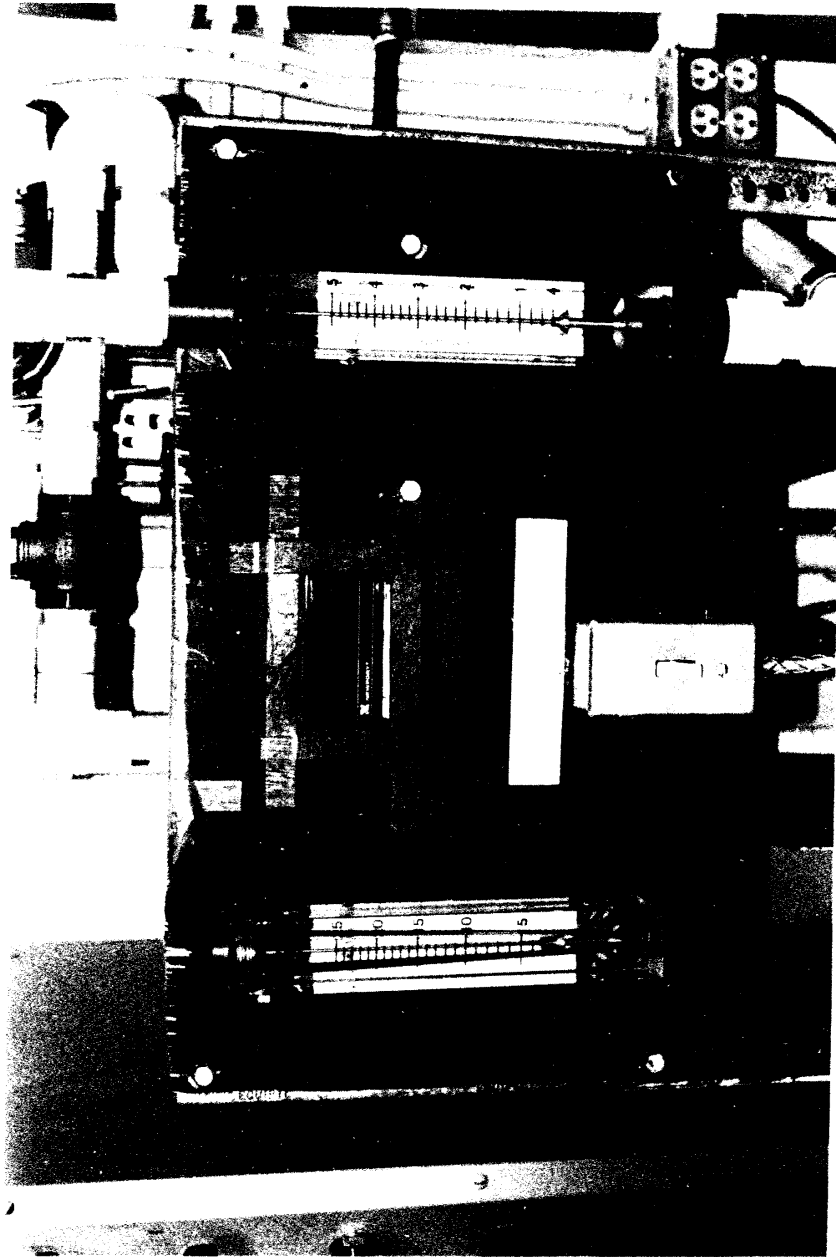
Figure 8. Photograph of the Front View of the Experimental Apparatus.

Signal Conditioner

Pin No.
1 Line (+)
2 Ground
3 Line (-)
4 Channel B
5 Channel A
6 Signal Common
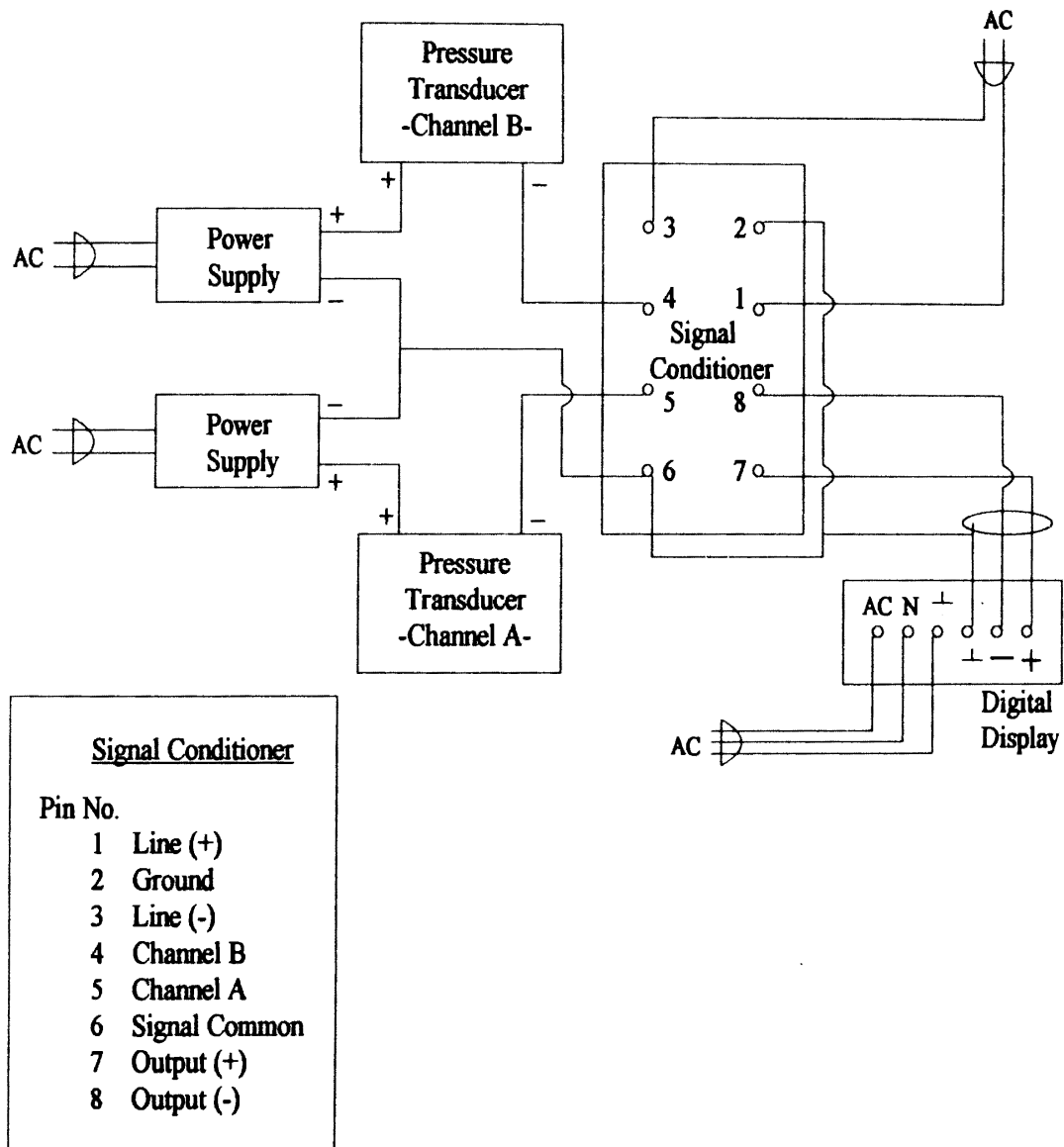7 Output (+)
8 Output (-)

Figure 9. Circuit Diagram Showing the Electrical Connections for the Pressure Drop
Measurement System.

various flow patterns related to two-phase flow. High speed photographs were taken at different flow rates of air and water to capture the hydrodynamic details of each flow pattern. A schematic diagram of the optical arrangement is shown in Figure 10. A Minolta (3Xi) camera mounted on a tripod was used with a 50 mm lens and a close-up filter attachment (2X). A high speed black and white film (3600 ASA) was used. A black background was used to achieve best results with the black and white film. The two sources of light were arranged in such a way that there was minimum glare and the gas-liquid interface was clearly visible. The results of the observations from the photographs are discussed in the next chapter.

Measurements on the holdup were performed in order to calculate the void fraction of the two-phase flow. This task was accomplished with the help of solenoid valves provided at both ends of the test section. While the two phase mixture was travelling upwards, the valves were closed simultaneously to trap the fluid in the test section. The gate valve, provided as a tap, was used to measure the volumes of the liquid and gas trapped in the test section. The volume occupied by the residual liquid that cannot be drained (found between the solenoid valve at the lower end and the opening of the gate valve used for draining the liquid) was measured to be 97 ml. This value was determined by pouring measured amounts of liquid into the tube space from which the liquid would not be drained during the actual measurement of the holdup. The total volume of the column was determined to be equal to 3185 ml, using similar measurement techniques. Knowing these values, the volume of the gas phase in the holdup was calculated and hence the void fraction of the flow.

The differential pressure during the two-phase flow was measured using the measurement system described previously. The pressure measurement system was calibrated using a stagnant liquid column. The pressure drop was read directly from the digital display. The value on the display presents the total pressure drop in psi (lb_f/in^2). The results obtained are discussed in detail in the next chapter.
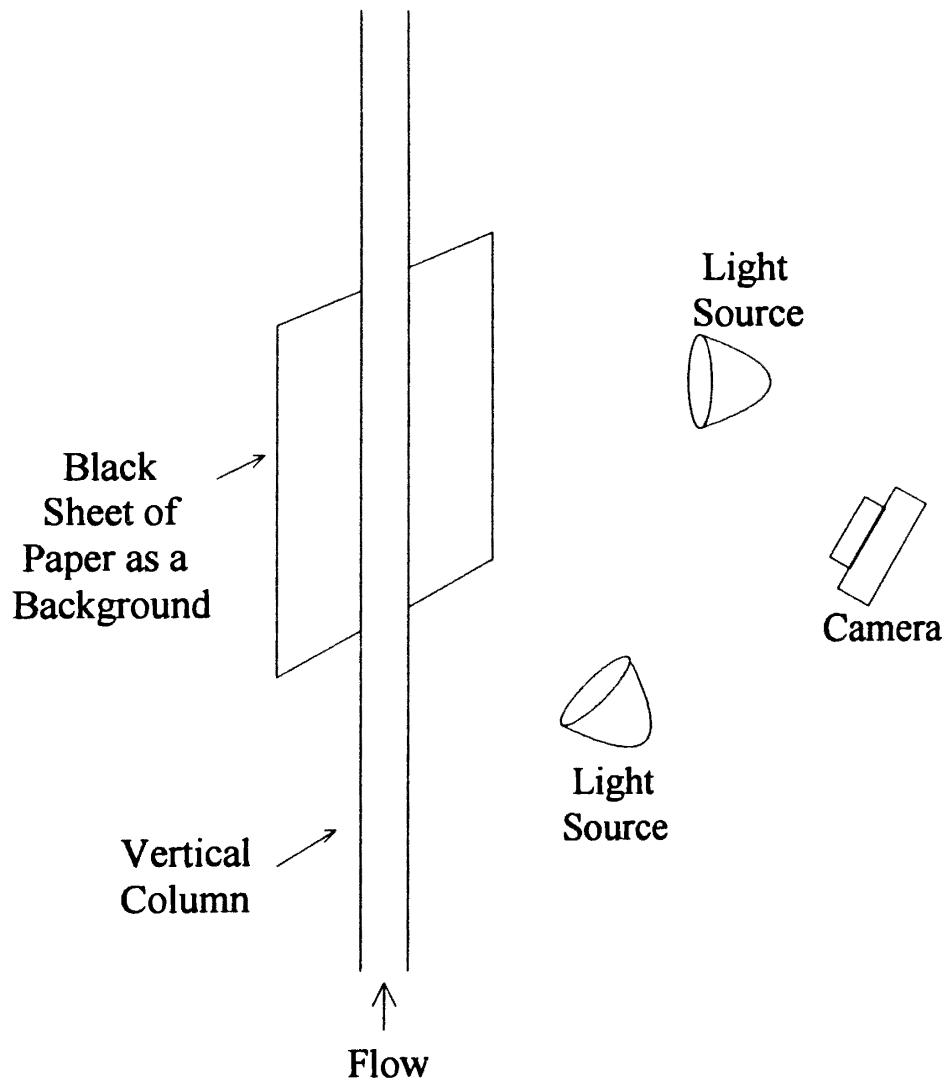
Figure 10.   Schematic Diagram of the Equipment Arrangement for Flow Pattern
            Visualization.

CHAPTER IV

RESULTS AND DISCUSSION

The observations and results, derived from experiments conducted using the apparatus constructed, are discussed in this chapter. Flow maps that indicate the different flow regimes of upward gas-liquid two-phase flow and charts to predict the two-phase variables, such as the void fraction of the flow and the pressure gradient along the vertical conduit, are presented. The results of this work are compared with those of previous researchers, and the observations are discussed.

Flow Visualization

The hydrodynamics of the gas-liquid two-phase flow is best visualized by high-speed photography. Some of the interesting observations from the photographs are presented. During bubbly flow, as shown in Figure 11, discrete bubbles were observed to travel in the liquid continuum as distorted spheres. With an increase in the gas flow rate, alternating Taylor bubbles and liquid slugs with small gas bubbles were observed. Figure 12 shows the tail portion of a Taylor bubble with a liquid slug containing many small gas bubbles following the Taylor bubble. The photograph in Figure 12 also shows the higher concentration of the gas bubbles near the tail of the Taylor bubble than in the rest of the liquid slug; this results from the entrainment of gas from the Taylor bubble into the liquid lug by the falling liquid film. Gas bubbles were occasionally observed in the falling liquid film, as demonstrated by the single gas bubble in Figure 13, which contradicts the

36

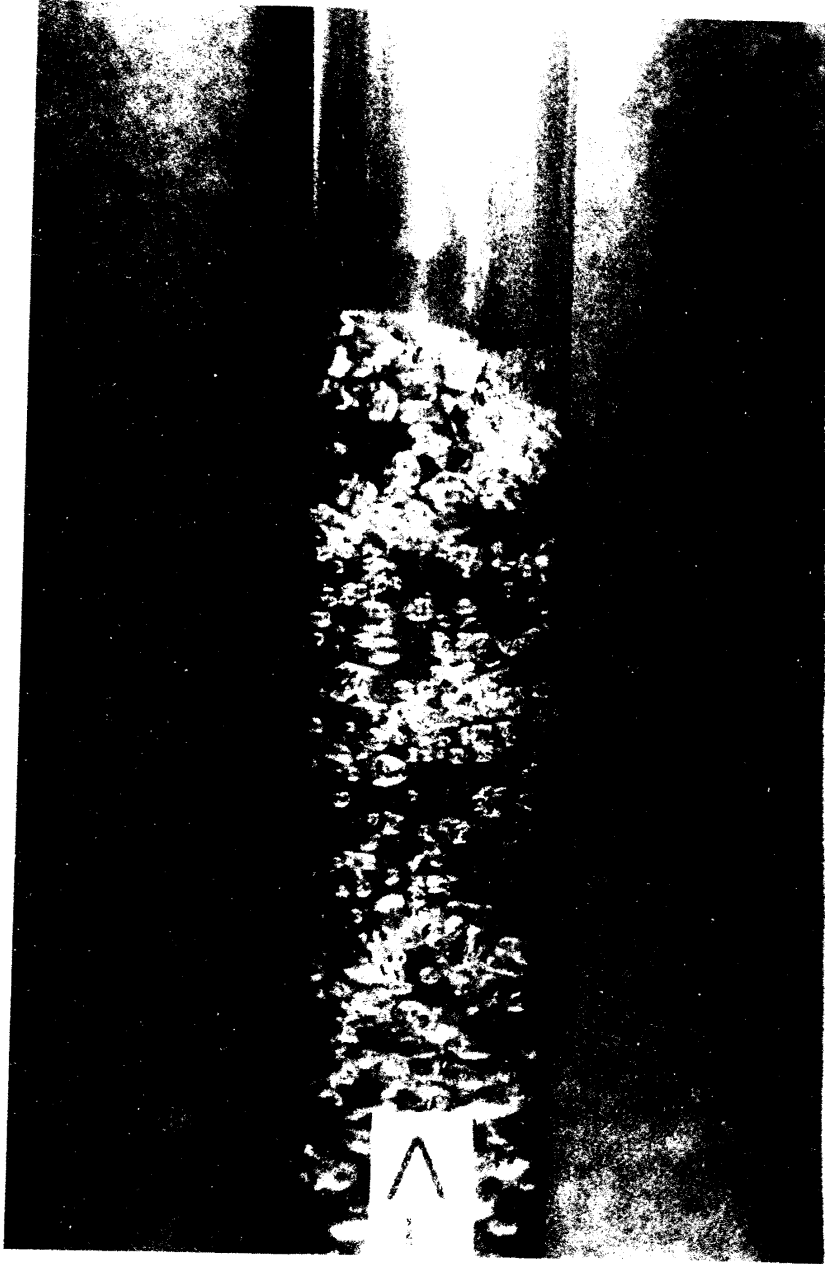Figure 11. Photograph of Bubbly Flow.

Figure 12. Photograph of Slug Flow.

Figure 13. Photograph Showing a Small Gas Bubble in the Falling Film During Slug Flow.

statement of Fernandes et al. (1983) that the liquid film is essentially bubble-free. The observation of bubbles in the falling liquid film during slug flow is also supported by the video tape produced by Rhodes (1982). The photograph in Figure 14 is most likely a picture of slug flow as the tail of the Taylor bubble can be seen with a high concentration of the small bubbles at the bottom end of the photograph. Although not very conclusive, the bubbles that are on the inner wall of the tube, as found in Figure 14, seem to be small bubbles in the liquid falling film around the Taylor bubble. However, the assumption of a bubble-free falling film is considered to be good enough for modeling purposes. When there was a considerable increase in the gas flow rate, the photograph of the flow (Figure 15) shows eddies in the liquid phase, indicating an upward and downward motion of the liquid, and hence the existence of churn flow in the column. At very high gas flow rates, the liquid film flowing along the inner wall of the tube, indicating annular flow, was clearly observed from the photograph shown in Figure 16. The photograph in Figure 16 indicates a wavy interface between the upward moving gas and liquid.

Flow Pattern Maps

Flow pattern maps were constructed to allow the prediction of flow regimes given the mass flow rates of the two fluids. A flow pattern map, as shown in Figure 17, was plotted with the liquid velocity as the abscissa and the gas velocity as the ordinate, both velocities having units of ft/s. The data used to plot this map are presented in Table I. Superficial velocities of the gas and liquid along with the corresponding flow pattern observed are presented in this table. Knowing the velocities of the two fluids flowing in the conduit, the flow regime that would occur at those velocities could be predicted from the map. With reference to the first row in Table I, when the gas velocity is constant at 9.2 ft/s and the liquid velocity is varied from 1.22 ft/s to 15.3 ft/s, the flow pattern observed is Churn. In order to compare this work's data with those obtained from

Figure 14. Photograph Showing Gas Bubbles in the Falling Film During Slug Flow.
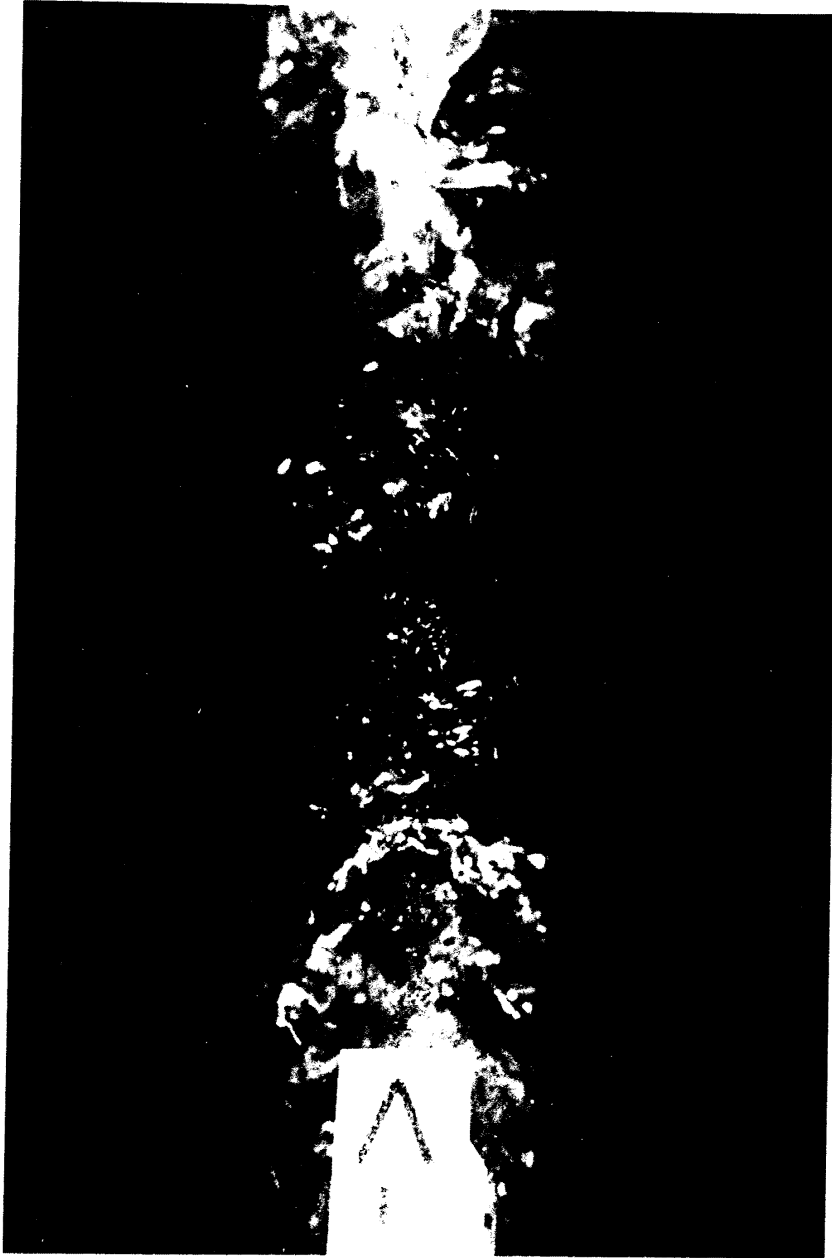
Figure 15. Photograph of Churn Flow.

Figure 16. Photograph of Annular Flow.
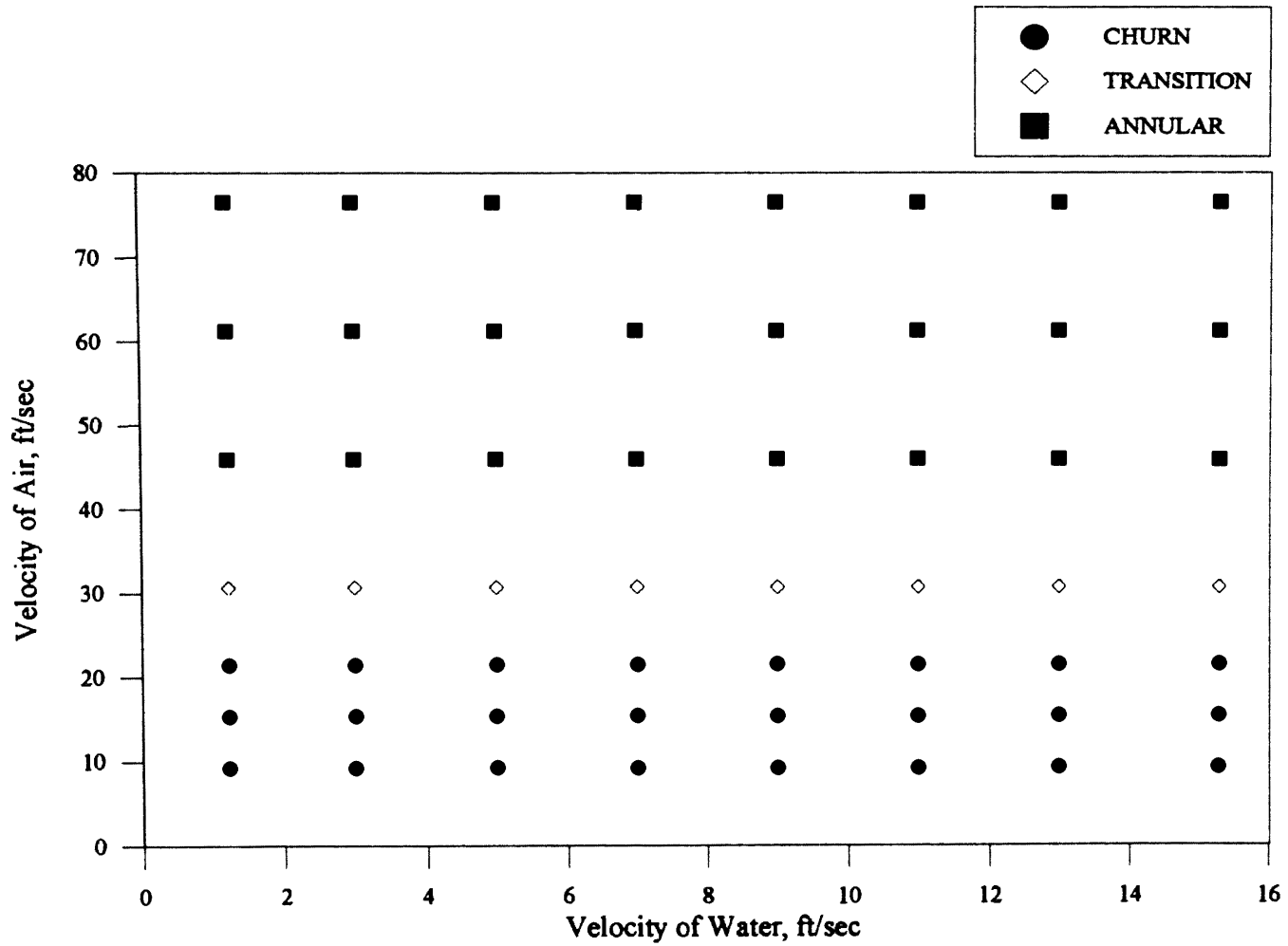
Figure 17.   Flow Regime Map Using Data from This Work.

TABLE I

DATA USED TO CONSTRUCT THE FLOW MAPS

Inside Diameter of the Tube = 1.029 inch

Pressure of Air = 20 psig

Velocity of Air $\overset{\bullet}{v}_g$ (ft/s)	Velocity of Water $\overset{\bullet}{v}_l$ (ft/s)	Flow Pattern
9.2	1.22 - 15.3	Churn
15.3	1.22 - 15.3	Churn
21.4	1.22 - 15.3	Churn
30.6	1.22 - 15.3	Transition
45.9	1.22 - 15.3	Annular
61.2	1.22 - 15.3	Annular
76.5	1.22 - 15.3	Annular

previous work, the data were plotted on the flow pattern map developed by Fair (1960) as

shown in Figure 18. Fair (1960) has considered churn flow as a short transition from slug

flow to the churn flow. Figure 18 indicates that the slug flow regime in the map

developed by Fair(1960) actually represents churn flow observed in this work. Mao et al.

(1993) supported Fair's work by arguing that the churn flow is a manifestation of slug

flow. This subject had been discussed in Chapter II. The present work accords with the

views of Hewitt et al. (1993) in the consideration of the churn flow as a separate flow

regime (also discussed in Chapter II). The slug flow regime could be assumed to lie to the

left of the churn flow regime in the map. The region further left would indicate bubbly

flow.

The bubbly and slug flow regimes are not indicated in the map in Figure 18 as the

corresponding flow rates of air and water could not be measured using the available range

of the rotameters. It should also be kept in mind that the lines separating the flow regimes

are not as sharp as in Figure 18, and are only meant to represent a broad transition band

lying between any two flow regimes on the map.

Void Fraction

A method was used to measure the liquid holdup in order to calculate the void

fraction of the flow as a function of the gas and liquid flow rates. The void fraction was

determined using the values of the total volume of the test section and the volume

measured using the gate valve provided at the bottom of the column, as described in the

last chapter.

The void fractions calculated from the holdup data of this work are presented in

Table II. A better perspective of the data was achieved by comparing the void fractions

calculated using the measured holdup with the modified Martinelli-Nelson graph plotted as

a function of the Martinelli parameter and the volume fractions of the two phases in the
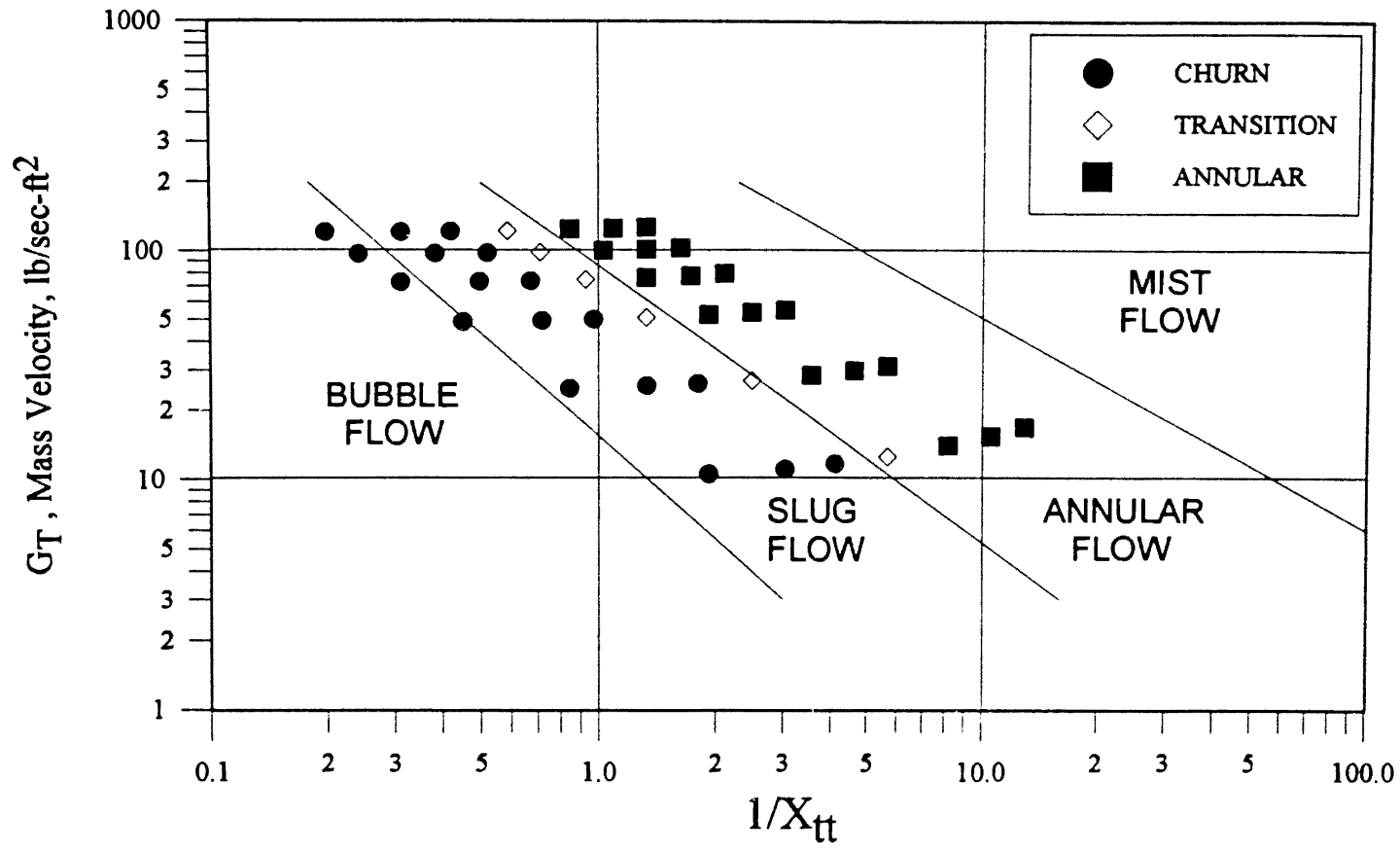
Figure 18. Comparison of This Work's Data with the Map Developed by Fair (1960).
[The Inclined Lines Representing Transitions are from Fair (1960)
and the Data are from This Study].

TABLE II

VOID FRACTION MEASUREMENTS OF GAS-LIQUID TWO-PHASE FLOW

Reduced Pressure of Air = 0.08

$\dot{V}_g$ (scfm)	$\dot{V}_l$ (gpm)	$\sqrt{\chi_{tt}}$	Water Holdup (ml)	R_v (Calculated)	R_v (Measured)	Flow Pattern
5	2	0.98	665	0.73	0.76	Churn
5	3	1.19	720	0.71	0.74	Churn
5	4	1.37	800	0.67	0.72	Churn
10	2	0.69	430	0.81	0.83	Annular
10	3	0.84	540	0.78	0.80	Annular
10	4	0.97	670	0.73	0.76	Churn
15	2	0.56	320	0.85	0.87	Annular
15	3	0.69	440	0.81	0.83	Annular
15	4	0.79	510	0.79	0.81	Annular
20	2	0.49	240	0.87	0.89	Annular
20	3	0.59	350	0.84	0.86	Annular
20	4	0.69	450	0.81	0.83	Annular

holdup (Bell, 1993). This work's data agreed quite well with the Martinelli-Nelson plot (Figure 5), as illustrated in Figure 19. The values of the volumetric flow rates, the values of $\sqrt{\chi_{tt}}$ calculated from the flow rates, the values of the void fraction obtained from the modified Martinelli-Nelson graph (Figure 5), and the values of void fraction calculated from the measured liquid holdup are presented in Table II. For an example calculation of the void fraction of the two-phase flow using the value of the measured liquid holdup as well as a calculation using the modified Martinelli-Nelson graph (Figure 5), refer to Appendix B.

Pressure Drop

Data on the total pressure drop due to two-phase flow were obtained using a measurement system described in Chapter III. Table III presents a sample set of data. Appendix C contains the remaining pressure drop data obtained by this work. The data of this work were compared with the values obtained from the sum of frictional pressure drop prediction of the Martinelli correlation, and the hydrostatic pressure drop calculated using the value of void fraction obtained from Figure 5. The comparisons are shown in Figures 20 through 22. The abscissas of the figures represent the air-water volume ratio of the flow, which is another way of quantifying the void fraction. The air-water volume ratios for this work's data were calculated from the experimental values of void fractions. For the case of the values to which this work's data are compared to, the air-water ratios were calculated using the void fraction values obtained from Figure 5.

It is well known that the Martinelli correlation underpredicts the measured pressure drop in most cases. The Martinelli correlation underpredicted the data obtained from this work by 50 to 80 %. The Martinelli correlation has been reported to perform poorly in the annular flow regime (Hewitt et al., 1963). The Martinelli correlation predictions were shown to be good, however, when a jet injector was used.
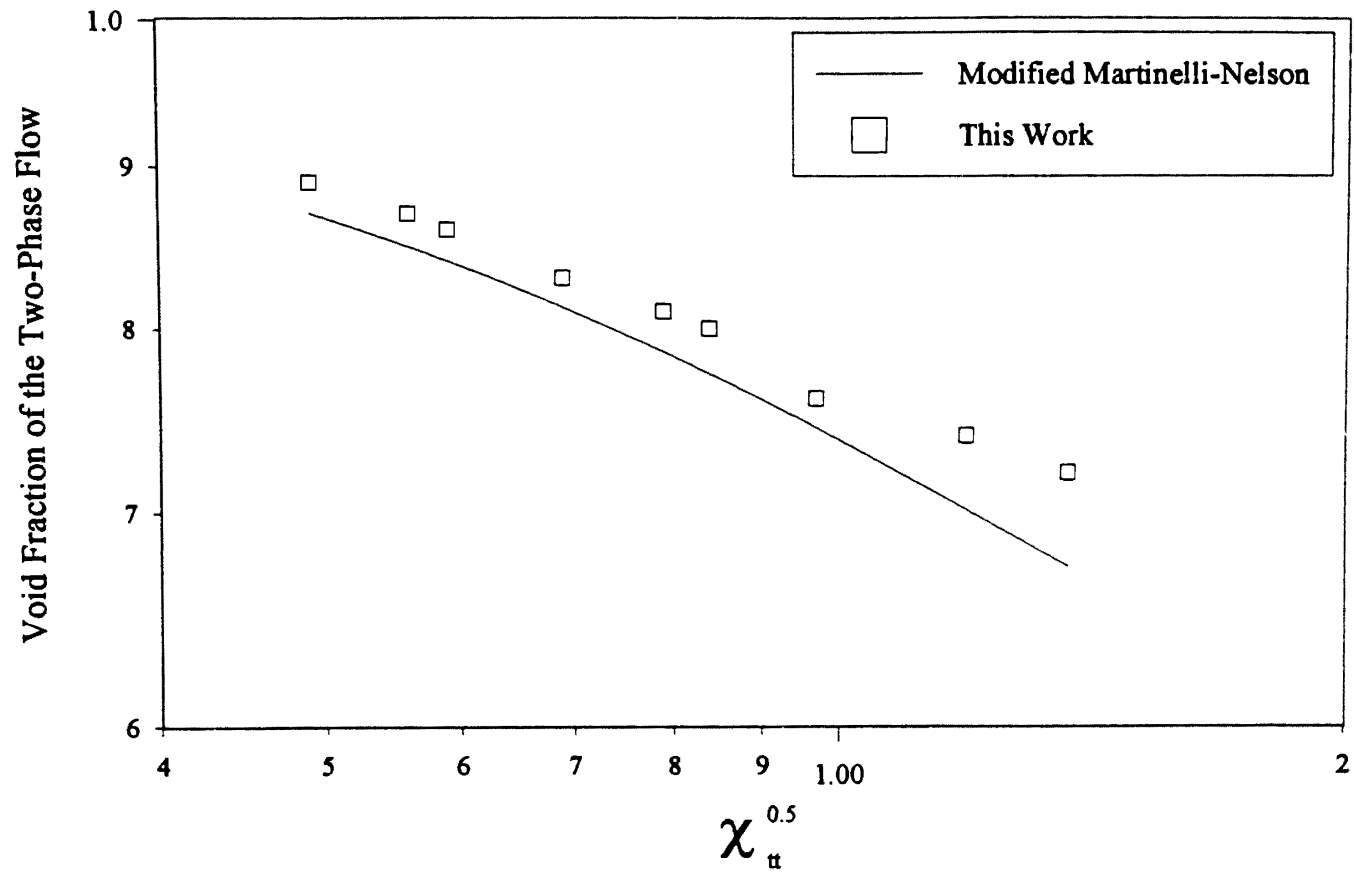
Figure 19. Comparison of This Work's Data on the Void Fraction of the Two-phase Flow
with the Modified Martinelli-Nelson Correlation (Figure 5).

TABLE III

PRESSURE DROP DATA DURING TWO-PHASE FLOW

$\dot{V}_l$ (gpm)	$\dot{V}_g$ (scfm)	Calculated Air-Water Ratio	Measured Air-Water Ratio	Calculated Pressure Drop ($lb_f/ft^2/ft$)	Measured Pressure Drop ($lb_f/ft^2/ft$)	Flow Pattern
2	5	2.70	3.20	-21.0	-54.7	Churn
2	10	4.30	4.88	-18.9	-63.8	Annular
2	15	5.67	6.70	-21.0	-86.6	Annular
2	20	6.70	8.10	-24.0	-106.6	Annular

Figure 20. Comparison of Pressure Drop Data of This Work with the Values Calculated from the Martinelli-Nelson Correlation at Volumetric Flow Rate of Water = 2 gpm.

Figure 21. Comparison of Pressure Drop Data of This Work with the Values Calculated from the Martinelli-Nelson Correlation at Volumetric Flow Rate of Water = 3 gpm.
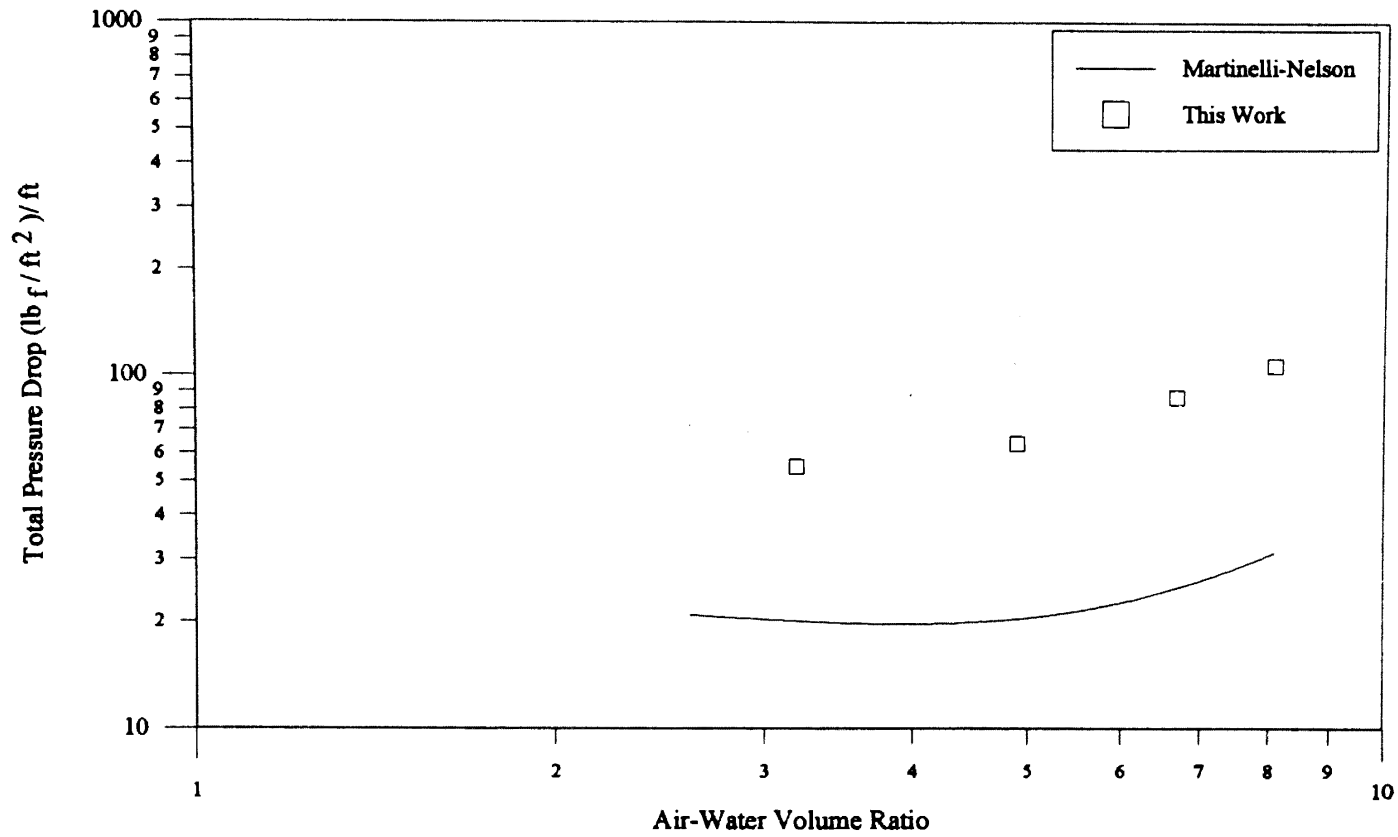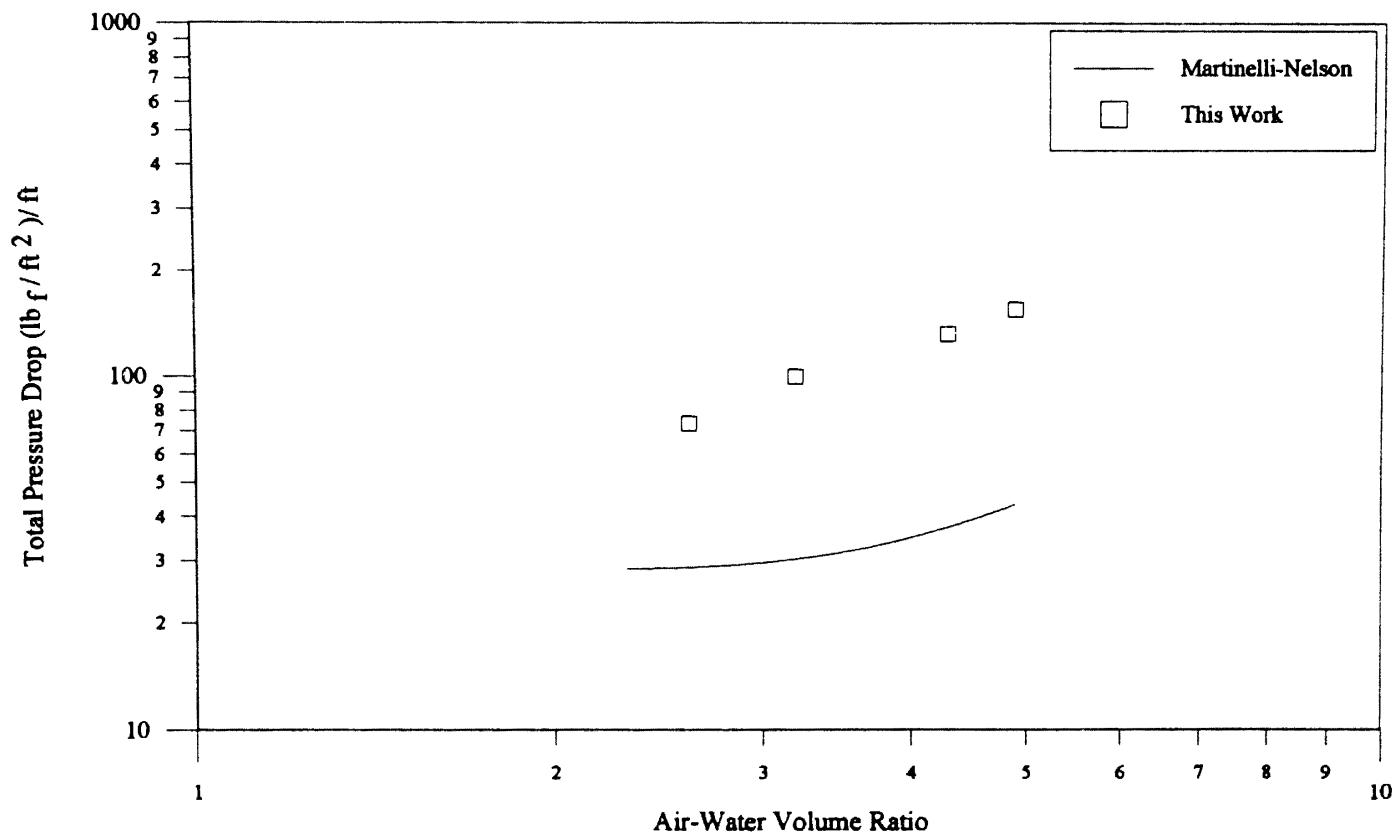
Figure 22. Comparison of Pressure Drop Data of This Work with the Values Calculated from the Martinelli-Nelson Correlation at Volumetric Flow Rate of Water = 4 gpm.
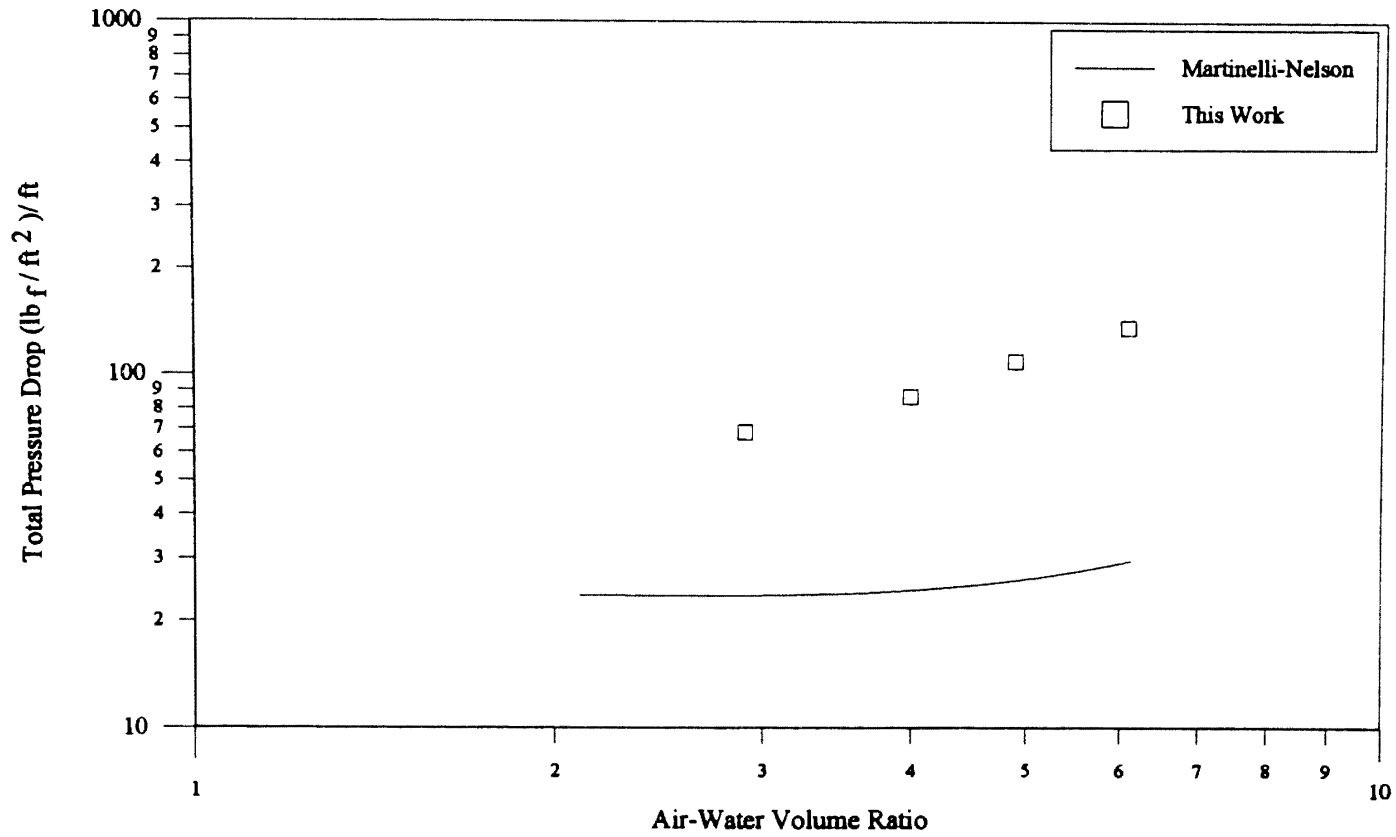
Hewitt et al. (1963) have referred to Bennett et al. (1961) who had used a jet injector and observed good agreement of their measurements with the predictions of Martinelli correlation. Hewitt et al. (1963) used an annular slot injector and reported that the Martinelli correlation underpredicted the pressure drops by a maximum of 75%. From the above discussion, it can be inferred that the injection mechanism significantly affects the pressure drop. Since this work used a mixing tee, the pressure drop was anticipated to be higher than the predictions, and the discrepancies between the data obtained in this work and the pressure drop values calculated using the Martinelli correlation seem reasonable.

CHAPTER V

CONCLUSIONS AND RECOMMENDATIONS

Conclusions

The major conclusions derived from this work are:

1. A safe and simple apparatus was designed to study the gas-liquid two-phase flow phenomenon. The flow pattern map developed by Fair (1960) worked quite well for design purposes.

2. An apparatus was successfully constructed to perform the desired functions, namely, visual observation of the flow patterns associated with vertical two-phase flow, and the measurement of void fraction of the flow and the pressure drop along the test section.

3. The various flow regimes were studied using visual observation and photographic techniques.

4. Provision for measuring the void fraction of the flow was included and the results have been shown to compare favorably with the Martinelli-Nelson predictions.

5. The Martinelli-Nelson correlation underpredicted the pressure drop data of this work by 50 to 80%. The reasonability of the underprediction was discussed in Chapter IV.

6. A limitation of this work, as in all the previous works, is the limited range of data that could be collected from the experimental apparatus built.

Recommendations

1. The major limitation of this work, the limited range of data collection, could be overcome by including flow meters that would measure very low flow rates of air.

2. Photographs could be used to obtain a rough estimate of the void fraction of the bubbly flow regime. This could be achieved by counting the number of bubbles per unit length of the column and calculating the volume fraction of the bubbles in the liquid continuum.

3. Different injection methods, such as jet injection and annular slot injection, could be tried to study the effect of the method of injection on the frictional pressure drop during the two-phase flow.

4. The diameter of the tube could be varied to study its effects on the parameters describing two-phase flow.

5. To better understand the annular flow, axial-view photography of the column could be used. An alternative would be to use a laser-sheet which would illuminate just the cross-section of the tube resulting in a better perspective of the film thickness.

6. Better correlations to predict the measured variables could be obtained for the void fraction and the pressure drop by using the experimental data provided by this work.

BIBLIOGRAPHY

Anderson, G. H. and Mantzouranis, B. G., "Two-Phase (Gas-Liquid) Flow Phenomena - I. Pressure Drop and Holdup for Two-Phase Flow in Vertical Tubes," *Chem. Eng. Sci.*, **12**, 109 (1960).

Baker, O., "Simultaneous Flow Oil and Gas," *Oil & Gas J.*, **53**, 185 (1954).

Bell, K. J., "Liquid-Gas/Vapor Two-Phase Flow," Class Notes for Process Heat Transfer, Section VIII, 1 (1993).

Bilicki, Z. and Kestin, J., "Transition Criteria for Two-Phase Flow Patterns in Vertical Upward Flow," *Int. J. Multiphase flow*, **13**, 283 (1987).

Brauner, N. and Barnea, D., "Slug/Churn Transition in Upward Gas-Liquid Flow," *Chem. Eng. Sci.*, **41**, 159 (1986).

Calvert, S. and Williams, B., "Upward Cocurrent Annular Flow of Air and Water in Smooth Tubes," *AIChE J.*, **1**, 78 (1955).

Chisholm, D., "Two-Phase Flow in Pipelines and Heat Exchangers," Pitman Press, London (1983).

DeJesus, J. M. and Kawaji, M., "Investigation of Interfacial Area and Void Fraction in Upward Cocurrent Gas-Liquid Flow," *Can. J. Chem. Eng.*, **68**, 904 (1990).

Fair, J. R., "What You Need to Design Thermosiphon Reboilers," *Pet. Ref.*, **39**, 105 (1960).

Fernandes, R. C., Semiat, R. and Dukler, A. E., "Hydrodynamic Model for Gas-Liquid Slug Flow in Vertical Tubes," *AIChE J.*, **29**, 981 (1983).

Galegar, W. C., Stovall, W. B. and Huntington, R. L., "More Data on Two-Phase Vertical Flow," *Pet. Ref.*, **33**, 208 (1954).

Golan, L. P. and Stenning, A. H., "Two-Phase Vertical Flow Maps," *Proc. Inst. Mech. Engrs.*, **184**, 108 (1969).

Govier, G. W., Radford, B. A. and Dunn, J. S. C., "The Upwards Vertical Flow of Air-Water Mixtures: I - Effect of Air-Water Rates on Flow Pattern, Holdup and Pressure drop," *Can. J. Chem. Eng.*, **35**, 58 (1957).

Govier, G. W. and Short, W. L., "The Upward Vertical Flow of Air-Water Mixtures: II - Effect of Tubing Diameter on Flow Pattern, Holdup and Pressure Drop," *Can. J. Chem. Eng.*, **36**, 195 (1958).

Hall-Taylor, N., Hewitt, G. F. and Lacey, P. M. C., "The Motion and Frequency of Large Disturbance Waves in Annular Two-Phase Flow of Air-Water Mixtures," *Chem. Eng. Sci.*, **18**, 537 (1963).

Hall-Taylor, N. S. and Nedderman, R. M., "The Coalescence of Disturbance Waves in Annular Two-Phase Flow," *Chem. Eng. Sci.*, **23**, 551 (1968).

Hewitt, G. F., "Disturbance Waves in Annular Two-Phase Flow," *Proc. Inst. Mech. Engrs.*, **184**, 142 (1969).

Hewitt, G. F. and Boure, J. A., "Some Recent Results and Developments in Gas-Liquid Flow: a Review," *Int. J. Multiphase Flow*, **1**, 139 (1973).

Hewitt, G. F. and Hall-Taylor, N. S., "Annular Two-Phase Flow," First edition, Pergamon Press, Oxford (1970).

Hewitt, G. F. and Jayanti, S., "To Churn or Not to Churn," *Int. J. Multiphase flow*, **19**, 527 (1993).

Hewitt, G. F., King, I. and Lovegrove, P. C., "Holdup and Pressure Drop Measurements in the Two-Phase Annular Flow of Air-Water Mixtures," *Brit. Chem. Eng.*, **8**, 31 (1963).

Jayanti, S. and Hewitt, G. F., "Prediction of the Slug-to-Churn Flow Transition in Vertical Two-Phase Flow," *Int. J. Multiphase flow*, **18**, 847 (1992).

Jayanti, S., Hewitt, G. F., Low, D. E. F. and Hervieu, E., "Observation of Flooding in the Taylor Bubble of Cocurrent Upwards Slug Flow," *Int. J. Multiphase flow*, **19**, 531 (1993).

Jepsen, J. C. and Ralph, J. L., "Hydrodynamic Studies of Two-Phase Upward Flow in Vertical Pipelines," *Proc. Inst. Mech. Engrs.*, **184**, 154 (1969).

Kabir, C. S. and Hasan, A. R., "Performance of a Two-Phase Gas/Liquid Flow Model in Vertical Wells," *J. Pet. Sci. & Eng.*, **4**, 273 (1990).

Kasturi, G., Stepanek, J. and Holland, F. A., "A Review of Two-Phase Flow Literature," *Brit. Chem. Eng.*, **16**, 333 and 511 (1970).

Lockhart, R. W. and Martinelli, R. C., "Proposed Correlation of Data for Isothermal Two-Phase, Two-Component Flow in Pipes," *Chem. Eng. Progress*, **45**, 39 (1949).

Mao, Z. S. and Dukler, A. E., "The Myth of Churn Flow?," *Int. J. Multiphase flow*, **19**,377 (1993).

Martinelli, R. C., Boelter, L. M. K., Taylor, T. H. M., Thomsen, E. G. and Morrin, E. H., "Isothermal Pressure Drop for Two-Phase Two-Component Flow in a Horizontal Pipe," *Trans. ASME*, **66**, 139 (1944).

Martinelli, R. C. and Nelson, D. B., Schenectady, N. Y., "Prediction of Pressure Drop During Forced-Circulation Boiling of Water," *Trans. ASME*, **70**, 695 (1948).

McQuillan, K. W. and Whalley, P. B., "Flow Patterns in Vertical Two-Phase Flow," *Int. J. Multiphase flow*, **11**, 161 (1985).

Nedderman, R. M. and Shearer, C. J., "The Motion and Frequency of Large Disturbance Waves in Annular Two-Phase Flow of Air-Water Mixtures," *Chem. Eng. Sci.*, **18**, 661 (1963).

Ragland, W. A., France, D. M. and Minkowycz, W. J., "Two-Phase Flow at the Flooding Point in an Annulus," *Exp. Thermal & Fluid Sci.*, **2**, 7 (1989).

Rhodes, E., "Gas-Liquid Flow," (on video tape), Heat Transfer & Fluid Flow Services, Atomic Energy Research Establishment, Harwell, England (1982).

Taitel, Y., Bornea, D. and Dukler, A. E., "Modelling Flow Pattern Transitions for Steady Upward Gas-Liquid Flow in Vertical Tubes," *AIChE J.*, **26**, 345 (1980).

Taitel, Y. and Dukler, A. E., "A Model for Predicting Flow Regime Transitions in Horizontal and Near Horizontal Gas-Liquid Flow," *AIChE J.*, **22**,47 (1976).

Tong, L. S., "Boiling Heat Transfer and Two-Phase Flow," John Wiley and sons, New York (1965).

Wallis, G. B. and Makkenchery, S., "The Hanging Film Phenomenon in Vertical Annular Two-Phase Flow," *Trans. ASME*, 297 (1974).

APPENDIXES

APPENDIX A

PHYSICAL PROPERTIES OF AIR AND WATER AND RELEVANT GEOMETRICAL DATA

Properties of Air:

Pressure of Air	$= 30 \text{ psig} = 44.7 \text{ psia} = 3.0 \text{ bar abs.}$
Critical Pressure of Air	$= 37.7 \text{ bar}$
Therefore, Reduced Pressure of Air	$= 0.08$
Density of Air at 25° C and 3 bar abs.	$= 0.22 \text{ lb}_m/\text{ft}^3$
Viscosity of Air at 25° C	$= 1.24 \times 10^{-5} \text{ lb}_m/\text{ft-sec}$

Properties of Water:

Density of Water at 25° C	$= 62.3 \text{ lb}_m/\text{ft}^3$
Viscosity of Water at 25° C	$= 6.72 \times 10^{-4} \text{ lb}_m/\text{ft-sec}$

Geometrical Data:

Internal Diameter of the Tube	$= 1.029 \text{ inch}$
Area of Cross-section of the Tube	$= 5.78 \times 10^{-3} \text{ ft}^2$
Height of the Column (Between the Two Pressure Taps)	$= 15.8 \text{ ft}$

APPENDIX B

EXAMPLE CALCULATION OF VOID FRACTION OF THE TWO-PHASE FLOW

Void Fraction of the Two-phase Flow Using the Modified Martinelli-Nelson Graph:

Volumetric Flow Rate of Air, $\dot{V}_g$ = 5 ft³/min, at 25°C and 3 bar abs.

Volumetric Flow Rate of Water, $\dot{V}_l$ = 2 gpm = 0.27 ft³/min

Mass Flow Rate of Air, $\dot{m}_g$ = $\dot{V}_g \cdot \rho_g$

$$= 5\left(\frac{ft^3}{min}\right)\left(\frac{1\,min}{60\,sec}\right)\left(\frac{0.22\,lb}{ft^3}\right)$$

$$= 0.018 \text{ lb/s}$$

Mass Flow Rate of Water, $\dot{m}_l$ = $\dot{V}_l \cdot \rho_l$

$$= 0.27\left(\frac{ft^3}{min}\right)\left(\frac{1\,min}{60\,sec}\right)\left(\frac{62.3\,lb}{ft^3}\right)$$

$$= 0.28 \text{ lb/s}$$

$$\chi_{tt} = \left(\frac{\dot{m}_l}{\dot{m}_g}\right)\left(\frac{\rho_g}{\rho_l}\right)^{0.57}\left(\frac{\mu_l}{\mu_g}\right)^{0.11} = \left(\frac{0.28}{0.018}\right)\left(\frac{0.22}{62.3}\right)^{0.57}\left(\frac{6.72\times10^{-4}}{1.24\times10^{-5}}\right)^{0.11}$$

$$= 0.96$$

$$\sqrt{\chi_{tt}} = 0.98$$

From Figure 5, at $P_r = 0.08$,

$$R_v = 0.73$$

Void Fraction of the Two-phase Flow from the Measured Liquid Holdup:

Volume of the residual water $= 97$ ml

Let the volume of water collected
    through the tap $= V$ ml

Total volume of the column $= 3185$ ml
    (between the quick-closing valves)

Volume of liquid in the holdup $= (97 + V)$ ml

Volume of gas in the holdup $= 3185 - (97 + V)$

Hence, the void fraction, R_v $= \dfrac{3185 - (97 + V)}{3185}$

For $V = 665$, R_v $= \dfrac{3185 - (97 + 665)}{3185}$

$= 0.76$

APPENDIX C

PRESSURE DROP DATA

$\dot{V}_l$ (gpm)	$\dot{V}_g$ (scfm)	Calculated Air-Water Ratio	Measured Air-Water Ratio	Calculated Pressure Drop ($lb_f/ft^2/ft$)	Measured Pressure Drop ($lb_f/ft^2/ft$)	Flow Pattern
3	5	2.1	2.9	-23.5	-68.4	Churn
3	10	3.0	4.0	-23.7	-86.6	Annular
3	15	3.8	4.9	-26.0	-109.4	Annular
3	20	4.6	6.1	-29.5	-136.7	Annular
4	5	2.3	2.6	-28.0	-73.0	Churn
4	10	2.6	3.2	-29.9	-99.4	Annular
4	15	3.2	4.3	-31.8	-132.2	Annular
4	20	3.8	4.9	-37.3	-155.0	Annular

APPENDIX D

EXAMPLE CALCULATION OF PRESSURE DROP
DURING THE TWO-PHASE FLOW

Volumetric Flow Rate of Air, $\dot{V}_g$ = 5 ft³/min, at 25°C and 3 bar abs.

Volumetric Flow Rate of Water, $\dot{V}_l$ = 2 gpm = 0.27 ft³/min

Mass Flow Rate of Air, $\dot{m}_g$

$$= \dot{V}_g \cdot \rho_g$$

$$= 5\left(\frac{ft^3}{min}\right)\left(\frac{1\,min}{60\,sec}\right)\left(\frac{0.22\,lb}{ft^3}\right)$$

$$= 0.018 \text{ lb/s}$$

Mass Flow Rate of Water, $\dot{m}_l$

$$= \dot{V}_l \cdot \rho_l$$

$$= 0.27\left(\frac{ft^3}{min}\right)\left(\frac{1\,min}{60\,sec}\right)\left(\frac{62.3\,lb}{ft^3}\right)$$

$$= 0.28 \text{ lb/s}$$

Liquid Mass Velocity, $G_l = \dfrac{\dot{m}_l}{S} = \dfrac{0.28\left(\dfrac{lb}{sec}\right)}{5.78 \times 10^{-3}\left(ft^2\right)}$

$$= 48.4 \text{ lb/ft}^2\text{-s}$$

$$Re_l = \frac{D_i G_l}{\mu_l} = \frac{\left(\frac{1.029}{12}\right)48.4}{6.72 \times 10^{-4}} \left(\frac{ft \cdot \left(\frac{lb}{ft^2 - sec}\right)}{\frac{lb}{ft - sec}}\right) = 6180$$

$$f_l = \frac{0.079}{(Re)^{1/4}} = \frac{0.079}{(6180)^{1/4}} = 8.91 \times 10^{-3}$$

$$\left(\frac{dp}{dl}\right)_{f,l} = -\frac{2 f_l G_l^2}{g_c D_i \rho_l}$$

$$= -\frac{2(8.91 \times 10^{-3})(48.4)^2}{32.2(0.0858)(62.3)} \left[\frac{\left(\frac{lb_m}{ft^2 - sec}\right)^2}{\left(\frac{lb_m - ft}{lb_f - sec^2}\right)(ft)\left(\frac{lb_m}{ft^3}\right)}\right]$$

$$= -0.24 \quad lb_f/ft^2/ft.$$

$$\chi_{tt} = \left(\frac{\dot{m}_l}{\dot{m}_g}\right)\left(\frac{\rho_g}{\rho_l}\right)^{0.57}\left(\frac{\mu_l}{\mu_g}\right)^{0.11} = \left(\frac{0.28}{0.018}\right)\left(\frac{0.22}{62.3}\right)^{0.57}\left(\frac{6.72 \times 10^{-4}}{1.24 \times 10^{-5}}\right)^{0.11}$$

$$= 0.96$$

$$\sqrt{\chi_{tt}} = 0.98$$

From Figure 5, at $P_r = 0.08$,

$$R_v = 0.73$$

From Figure 6, at $P_r = 0.08$,

$$\Phi_{tt} = 4.1$$

$$\left(\frac{dp}{dl}\right)_{f,TPF} = \Phi_{lu}^2 \cdot \left(\frac{dp}{dl}\right)_{f,l}$$

$$= (4.1)^2 (-0.24)$$

$$= -4.03 \quad lb_f/ft^2/ft.$$

$$\rho_{eff} = R_v \rho_g + (1 - R_v)\rho_l$$

$$= (0.73)(0.22) + (0.27)(62.3)$$

$$= 16.98 \quad lb_m/ft^3$$

$$\left(\frac{dp}{dl}\right)_{g,TPF} = -\rho_{eff} \frac{g}{g_c} Cos\theta$$

$$= -(16.98)\left(\frac{32.2}{32.2}\right)Cos0$$

$$= -16.98 \quad lb_f/ft^2/ft.$$

$$\left(\frac{dp}{dl}\right)_{T,TPF} = \left(\frac{dp}{dl}\right)_{f,TPF} + \left(\frac{dp}{dl}\right)_{g,TPF}$$

$$= -4.03 - 16.98$$

$$= -21.01 \quad lb_f/ft^2/ft.$$

APPENDIX E

LIST OF COMPONENTS USED IN THE EXPERIMENTAL WORK

Part No.	Name of the component	No. of items	Model No.	Manufacturer
1	Air Rotameter	1	FR 5000S	Key Instruments
2	Water Rotameter	1	FR 5000I	Key Instruments
3	Globe Valves	2	4600K15	McMaster-Carr
4	Needle Valve	1	EA40608	Ace Hardware
5	Ball Valve	1	17105K85	McMaster-Carr
6	Gate Valves	3	EA4403	Ace Hardware
7	Check Valve (water line)	1		Ace Hardware
8	Check Valve (air line)	1	9770K45	McMaster-Carr
9	Transparent PVC Pipe		Excelon R-4000	Cope Plastics
10	PVC Sch. 40 Pipes		EA44154	Ace Hardware
11	PVC Pipe Fittings and Other Accessories			Ace Hardware
12	Pressure Transducers	2	C207	SETRA
13	Power Supply	3	867	Beckman Industrial

List of Components: Contd.

Part No.	Name of the component	No. of items	Model No.	Manufacturer
14	Signal Conditioner (Subtraction Module)	1	8000	Beckman Industrial
15	Digital Display	1	202A	Newport Electronics Inc.

VITA

Nambi Shanmugam

Candidate for the Degree of

Master of Science

Thesis: UPWARD CO-CURRENT GAS-LIQUID TWO-PHASE FLOW IN VERTICAL TUBES

Major Field: Chemical Engineering

Biographical:

    Personal Data: Born in Madurai, India, October 2, 1970, the son of Shanmugam AR. and Mariammal S.

    Education: Received Bachelor of Technology Degree in Chemical Engineering from Bharathiar University at Coimbatore in May, 1992; completed requirements for the Master of Science degree at Oklahoma State University in May, 1994.

    Professional Experience: Teaching Assistant, Department of Chemical Engineering, Oklahoma State University, August, 1992, to May, 1993; Research Assistant, Department of Chemical Engineering, Oklahoma State University, June, 1993, to December, 1993; Laboratory Monitor, CEAT Computer Laboratories, Oklahoma State University, January, 1994, to May, 1994.